HHS Public Access

Author manuscript

J Comp Neurol. Author manuscript; available in PMC 2019 October 15.

Published in final edited form as:

J Comp Neurol. 2018 October 15; 526(15): 2444–2461. doi:10.1002/cne.24504.

Prss56 expression in the rodent hypothalamus: Inverse correlation with proopiomelanocortin suggests oscillatory gene expression in adult rat tanycytes

Gábor Wittmann[1] and **Ronald M. Lechan**[1,2]

[1]Department of Medicine, Division of Endocrinology, Diabetes and Metabolism, Tupper Research Institute, Tufts Medical Center, Boston, MA 02111, USA

[2]Department of Neuroscience, Tufts University School of Medicine, Boston, MA 02111, USA

Abstract

We recently reported that the number of hypothalamic tanycytes expressing proopiomelanocortin (*Pomc*) is highly variable among brains of adult rats. While its cause and significance remain unknown, identifying other variably expressed genes in tanycytes may help understand this curious phenomenon. In this *in situ* hybridization study, we report that the *Prss56* gene, which encodes a trypsin-like serine protease and is expressed in neural stem/progenitor cells, shows a similarly variable mRNA expression in tanycytes of adult rats and correlates inversely with tanycyte *Pomc* mRNA. *Prss56* was expressed in α1, β1, subsets of α2, and some median eminence γ tanycytes, but virtually absent from β2 tanycytes. *Prss56* was also expressed in vimentin positive, tanycyte-like cells in the parenchyma of the ventromedial and arcuate nuclei, and in thyrotropin beta subunit-expressing cells of the pars tuberalis of the pituitary. In contrast to adults, *Prss56* expression was uniformly high in tanycytes in adolescent rats. In mice, *Prss56*-expressing tanycytes and parenchymal cells were also observed but fewer in number and without significant variations. The results identify *Prss56* as a second gene that is expressed variably in tanycytes of adult rats. We propose that the variable, inversely correlating expression of *Prss56* and *Pomc* reflect periodically oscillating gene expression in tanycytes rather than stable expression levels that vary between individual rats. A possible functional link between Prss56 and POMC, and *Prss56* as a potential marker for migrating tanycytes are discussed.

Keywords

ependyma; vimentin; glial fibrillary acidic protein; Ki-67 antigen; neurogenesis; periodicity; RRID:AB_221448; RRID:AB_2216104; RRID:AB_2109815; RRID:AB_442102; RRID:AB_514500; RRID:AB_2532342; RRID:AB_840257; RRID:SCR_002285; RRID:SCR_003070

Corresponding author: Gábor Wittmann, PhD or Ronald M. Lechan, MD, PhD, Department of Medicine, Division of Endocrinology, Diabetes and Metabolism, Tufts Medical Center, #268, 800 Washington Street, Boston, Massachusetts, 02111, Phone: 617-616-0117, Fax: 617-636-4719, gwittmann@tuftsmedicalcenter.org or rlechan@tuftsmedicalcenter.org.

Introduction

Pro-opiomelanocortin (POMC) is a critically important regulatory protein acting both as a hormonal and a neurotransmitter precursor: adrenocorticotropin (ACTH) released from pituitary corticotrophs regulates corticosteroid production of the adrenal gland, while α-melanocyte-stimulating hormone (α-MSH) released from hypothalamic neurons regulates food intake and energy expenditure (Cawley, Li, & Loh, 2016). In rats, *Pomc* is also expressed in hypothalamic tanycytes (Baubet et al., 1994; Larsen & Mau, 1994; Lu et al., 2002; Ross et al., 2009; Ross et al., 2015; Sergeyev, Vegeyeva, & Akmayev, 2011; Willesen, Kristensen, & Romer, 1999; Wittmann et al., 2017), ependymoglial cells that reside in the ventrolateral wall and floor of the caudal third ventricle and also within the median eminence and infundibular stalk (Wittkowski, 1998; Wittmann et al., 2017). The function of POMC in tanycytes is not yet understood. We recently reported the curious phenomenon that there are marked differences among adult rats with respect to the number and distribution of POMC-expressing tanycytes (Wittmann et al., 2017). These differences are present at both the mRNA and protein levels, exist in both males and females and among rats with similar age and weight that were euthanized at the same time of the day (Wittmann et al., 2017). While the cause of this variability remains unknown, there are only two conceivable explanations for this phenomenon. One is individual variation among animals; the other is that POMC expression in tanycytes oscillates between low and high levels in each brain.

To better understand this phenomenon, we searched for other genes with similarly variable expression in tanycytes. As a first step, we screened the available literature, looking for descriptions and photographs that mention or indicate natural variability in tanycyte gene expression. While such obvious clues were not found, we came upon a unique expression pattern, that of *Prss56,* a trypsin-like serine protease (Nair et al., 2011), which is expressed specifically in neural stem/progenitor cells in the adult and embryonic mouse brain, including tanycytes (Jourdon et al., 2016). Reporter expression in $Prss5^{Cre/+}$,$Rosa2^{6tdTom}$ mice labels tanycytes, but only a fraction of them in aseemingly random distribution, as well as tanycyte-like cells in the hypothalamic parenchyma that appear to be former tanycytes that translocated their soma into the parenchyma (Jourdon et al., 2016). Based on this unusual pattern, we hypothesized that *Prss56* is expressed transiently in mouse tanycytes, and therefore, a potential candidate for a variably expressed gene that correlates with *Pomc* in rat tanycytes. To examine this possibility, we characterized *Prss56* expression using *in situ* hybridization (ISH) in both the rat and mouse hypothalamus.

Materials and Methods

Animals

Male and female Sprague-Dawley rats (Taconic Farms, Germantown, NY) and C57Bl/6 mice (Taconic) were housed under standard conditions (12h light/dark cycle, temperature between 20 to 24 °C, rodent chow, and water *ad libitum).* In total, 30 rats and 18 mice were used in this study; the body weights/ages are included in Table 1 and in the Results. All experimental protocols were reviewed and approved by the Institutional Animal Care and Use Committee at Tufts Medical Center.

Tissue preparation for fluorescent in situ hybridization (FISH)

The animals were deeply anesthetized with ketamine-xylazine (ketamine: 75 mg/kg; xylazine: 10 mg/kg body weight) and then decapitated. The brains were removed and snap-frozen on powdered dry ice. Then, 18 μm (for rats) or 16 μm (for mice) thick coronal sections were cut through the entire extent of the hypothalamic arcuate nucleus using a Leica CM3050 S cryostat (Leica Microsystems, Nussloch GmbH, Germany), thaw-mounted on Superfrost Plus glass slides (Fisher Scientific Co., Pittsburgh, PA), and air-dried. Rat hypothalamic sections were collected in 1-in-12 series on a total of 24 (2×12) slides per brain. With 6 hypothalamic sections on each slide, a series containing every 12th section fit on 2 slides, one containing the rostral, and another the caudal part of the tanycyte region. Mouse sections were collected in 1-in-14 series, with 6 to 8 sections on each slide. The sections were stored at −80°C until processed for FISH.

Riboprobe synthesis

A 1,000 bases long template DNA corresponding to 999–1998 of XM_003750730.4, predicted rat *Prss56* transcript variant X2 mRNA, was synthesized and cloned into pBluescript SK(−) plasmid by GenScript (Piscataway, NJ). This sequence is 94% identical to the corresponding region of mouse *Prss56* mRNA, NM_027084. The template for *Pomc* riboprobe was a 1008 bp DNA sequence, corresponding to mouse *Pomc* mRNA transcript variant 5, NM_001278584.1, synthesized and cloned into pBluescript SK(−) by GenScript. This sequence has a 93% homology to the rat *Pomc* mRNA, NM_139326.2. Antisense probes and the sense control transcript for *Prss56* were synthesized by *in vitro* transcription in the presence of digoxigenin-11-UTP (Roche Applied Sciences, Basel, Switzerland). For radioactive detection of *Prss56*, the antisense probe was synthesized using [35S]-uridine 5'-(alpha-thio) triphosphate (PerkinElmer), and purified with Mini Quick Spin RNA columns (Roche). The riboprobe for thyroid-stimulating hormone β subunit mRNA *(Tshb)* was synthesized in the presence of fluorescein-12-UTP (Roche) from a template corresponding to 8–512 of NM_013116.2, rat *Tshb* mRNA (kindly provided by Perry Barrett, Rowett Institute, University of Aberdeen, UK).

FISH combined with immunofluorescence

FISH for *Prss56* was performed on serial sections of all rats and mice used in this study, according to the protocol previously described for fresh frozen sections (Wittmann, Hrabovszky, & Lechan, 2013). Following the hybridization procedure, sections were treated with 0.5% Triton X-100/0.5% H_2O_2 in PBS (pH 7.4) for 15 min, rinsed in PBS, immersed in maleate buffer (0.1 M maleic acid, 0.15 M NaCl, pH 7.5; 10 min), and in 1% blocking reagent for nucleic acid hybridization (Roche). The sections were incubated overnight in peroxidase-conjugated sheep anti-digoxigenin antibody (Roche, Cat# 11207733910, RRID:AB_514500; diluted 1:100 in 1% blocking reagent) using CoverWell incubation chambers (Grace Bio-Labs Inc., Bend, OR). After rinses in PBS, the hybridization signal was amplified with the TSA Plus Biotin Kit (Perkin Elmer, Waltham, MA), by using 1:300 dilution of the TSA Plus biotin reagent in 0.05M Tris buffer (pH 7.6) containing 0.01% H_2O_2. The reaction was stopped after 30 min, and the sections were incubated in Alexa Fluor 488-conjugated Streptavidin (Thermo Fisher Scientific, Waltham, MA) for 2h, diluted

at 1:500 in 1% blocking reagent. The sections were further processed for immunofluorescence by incubating them in the mixture of chicken anti-vimentin antibody and one of the following antibodies: mouse anti-HuC/D antibody (2 brains from Group 3; 4 brains from Group 4, see Table 1; all adolescent rats and all mice); mouse anti-glial fibrillary acidic protein (GFAP) antibody (2 brains each from Groups 3&4); or a rabbit antibody against Ki-67 (Groups 1&2). The primary antibodies were detected with the following cocktails of secondary antibodies: Cy3- conjugated anti-chicken and Alexa Fluor 647-conjugated anti-mouse; Cy3-conjugated anti-mouse and Alexa 647-conjugated anti-chicken; and Cy3-conjugated anti-rabbit and Alexa 647-conjugated anti-chicken IgGs, respectively (all from Jackson Immunoresearch, West Grove, PA; 1:200 dilution each). Sections were coverslipped with Vectashield mounting medium containing DAPI (Vector Laboratories, Burlingame, CA).

To illustrate correlation with *Prss56,* FISH for *Pomc* was performed on adjacent sections of Groups 1 and 2 (Table 1) as described above, with the same signal amplification method.

Dual ISH for Prss56 and Pomc

An additional set of sections from Groups 1 and 2 (Table 1) were processed for combined radioactive ISH and FISH by mixing the [S-35]-labeled *Prss56* riboprobe (50,000 cpm/µ1 probe concentration) and the digoxigenin-labeled *Pomc* riboprobe. Following the final FISH detection step (Alexa Fluor 488-conjugated Streptavidin), sections were dehydrated in ascending series of ethanol, air-dried, and dipped into Kodak NTB autoradiography emulsion (Carestream Health Inc., Rochester, NY). The emulsion coated-slides were stored in light-tight boxes at 5°C for 28d, then the autoradiograms were developed using Kodak D-19 replacement developer (Electron Microscopy Sciences). Slides were dehydrated in ascending series of ethanol followed by xylenes (Sigma-Aldrich), and coverslipped with DPX mountant (Sigma-Aldrich).

Dual FISH for Prss56 and Tshb

Dual FISH was performed on sections from three adult rats, by mixing the digoxigenin-labeled *Prss56* and fluorescein-labeled *Tshb* probes. Following hybridization, sections were first incubated in the peroxidase-conjugated sheep anti-digoxigenin antibody, and the signal was amplified using the TSA Plus DIG Kit (Cat# NEL748E001KT, Perkin Elmer) for 30 min, applying the DIG amplification reagent at 1:500 dilution in 0.05M Tris (pH 7.6) containing 0.01% H_2O_2. Sections were then incubated in a rabbit monoclonal antibody against digoxigenin (Thermo Fisher, Cat# 700772, RRID:AB_2532342; at 1 µg/ml concentration) for 3h, in the presence of 2% sodium azide to inactivate peroxidase activity. Sections were thoroughly washed in PBS, and incubated overnight in peroxidase-conjugated sheep anti-fluorescein antibody (Roche, Cat# 11426346910, RRID:AB_840257; diluted 1:100 in 1% blocking reagent). Signal amplification was applied using the TSA Plus Biotin Kit as described above, and the signals were detected with the cocktail of Alexa Fluor 488-conjugated Streptavidin and Alexa 594-conjugated anti-rabbit IgG (Jackson; 1:200). The red and green fluorescence of Alexa 594 and Alexa 488, respectively, were swapped in the images to keep the green color consistent for *Prss56.*

Imaging

Images were captured with a Zeiss Axioplan 2 epifluorescent microscope (Carl Zeiss Ltd., Göttingen, Germany) equipped with a RT SPOT digital camera (Diagnostic Instruments, Sterling Heights, MI). Confocal images were captured with a Leica SPE confocal microscope. Z-projections of confocal image stacks were created by Fiji (http://fiji.sc; RRID:SCR_002285) (Schindelin et al., 2012). Adobe Photoshop CS4 (Adobe Systems Inc., San Jose, CA) was used to create and label composite images and to modify brightness and contrast to increase the visibility of lower level signals.

Quantification ISH signal, cell counts and statistics

To quantify FISH signal for *Prss56* in rats, sections were imaged with a 10× objective, then overlapping fields were merged using the Photomerge function of Photoshop CS4. Images were transformed to 8-bit grayscale mode, hybridization signal was separated from the background by the threshold function of ImageJ software (http://rsb.info.nih.gov/ij; RRID:SCR_003070) (Schneider, Rasband, & Eliceiri, 2012), and the area covered by hybridization signal was measured over the entire tanycyte region where specific labeling was observed. Hybridization signal was measured in every section (10–11 sections) from each 22 adult rat. *Prss56* hybridization signal over parenchymal cells was quantified in the same manner, but separately from tanycytes. To correlate *Prss56* expression with *Pomc* in tanycytes, *Pomc* hybridization signal was quantified from the same 22 brains on darkfield images of radioactive *Pomc* ISH from our previous study (Wittmann et al., 2013). *Pomc* hybridization signal was measured similarly, in every section from each brain, over the entire tanycyte region with specific hybridization signal, including the median eminence and infundibular stalk. The Pearson correlation coefficient was calculated using GraphPad Prism 4.0. *Prss56* hybridization signal of parenchymal cells was compared between groups by one-way ANOVA and Bonferroni's post-hoc test.

The number of parenchymal Prss56-expressing cells was counted in each section from 10 brains (Groups 3&4 in Table 1). To estimate the total number of these cells, correction for profile overcounting was applied using Abercrombie's formula (Guillery, 2002). Therefore, a correction factor of 0.76 was computed using the formula 18/(18+5.7), where 18 is section thickness μm), and 5.7 is the mean nuclear diameter of parenchymal *Prss56* cells (5.7 ± 0.2μm, n=50 cells). The percentage of parenchymal *Prss56*- expressing cells co-expressing vimentin or GFAP was calculated from 4 brains each. Data are presented as mean ± SEM. Ki-67 positive cells in the tanycytic ependyma and adjacent regions were counted on each section from 12 brains (Groups 1&2 in Table 1). In mice, Prss56-expressing tanycytes and parenchymal cells were counted on every section (6–7 section per brain).

Antibody characterization

The polyclonal chicken vimentin antibody (Millipore, Cat# AB5733, RRID:AB_2216104; used at 1:5K dilution) was raised against recombinant vimentin, and its specificity was confirmed by dual immunofluorescence with a mouse monoclonal vimentin antibody (Millipore, Cat# MAB3400, RRID:AB_94843), which resulted in complete colocalization (Wittmann et al., 2017). These two vimentin antibodies recognize different epitopes, as only the chicken, but not the mouse antibody recognizes murine vimentin. The mouse

monoclonal HuC/D antibody (Life Technologies, Cat# A21271, RRID:AB_221448; used at 1 μg/ml concentration) was raised against human HuC/D, has been well characterized and yielded the well-known pattern of neuronal cell bodies (Lee et al., 2012; Wittmann, Mohacsik, Balkhi, Gereben, & Lechan, 2015). The mouse monoclonal GFAP antibody (Millipore, Cat# MAB360, RRID:AB_2109815; used at 1:2K dilution) was raised against purified porcine GFAP, and labeled the majority of tanycytes in rats, consistent with previous reports (Chauvet, Privat, & Alonso, 1996; Perez-Martin et al., 2010; Zoli, Ferraguti, Frasoldati, Biagini, & Agnati, 1995). It is worth noting that detecting GFAP in rat tanycytes can highly depend on fixation and pretreatment conditions, as previously noted by others (Chauvet et al., 1996; Kawakami, 2000). In our experience, the same antibody at the same concentration labels only a small subset of tanycytes in sections from paraformaldehyde-perfused brains that were pretreated with 0.5% Triton X-100 (data not shown), whereas the conditions in the present study increased the sensitivity of GFAP detection. The rabbit polyclonal Ki-67 antibody (Leica Biosystems, NCL-Ki67p, RRID:AB_442102; used at 1:500 dilution) was raised against a recombinant fusion protein containing Ki-67 motif. This antibody labeled nuclei, consistent with the subcellular location of this antigen (Scholzen & Gerdes, 2000), the distribution of which was in agreement with previous studies of cell proliferation in the rat hypothalamus (see Results). The specificity of this antibody in our conditions was further confirmed by immunostaining sections from the same brains using a methanol fixation protocol (Wittmann, Szabon et al., 2015), which resulted in highly similar numbers and distribution of Ki-67-labeled nuclei.

Tanycyte nomenclature

For tanycytes that line the ventrolateral walls and floor of the third ventricle, we followed the original classification (α1, α2, β1 and β2 subtypes) by Akmayev and colleagues (Akmayev & Fidelina, 1976; Akmayev, Fidelina, Kabolova, Popov, & Schitkova, 1973). In rostral and caudal regions, where a horizontal ventricle floor is not present, tanycytes in the ventral tip of the ventricle were identified as β1 tanycytes in agreement with Rodriguez et al. (Rodriguez, Gonzalez, & Delannoy, 1979). An additional tanycyte subtype resides within the tissue of the median eminence/infundibular stalk, from below the layer of β2 tanycytes throughout the external zone. These cells were originally described in rats as astrocytic tanycytes (Bitsch & Schiebler, 1979; Rutzel & Schiebler, 1980; Zaborszky & Schiebler, 1978), and subsequently as subependymal tanycytes and pituicytes (Wittkowski, 1980, 1998) or just generally as tanycytes (Hokfelt et al., 1988; Kawakami, 2000; Meister et al., 1988). In the Mongolian gerbil they were called subependymal tanycytes and tanycyte-like cells in the external zone of the median eminence (Redecker, 1989a, 1989b, 1990). In our previous study, we integrated these cells into the Greek alphabetic nomenclature by giving them the name γ tanycytes (Wittmann et al., 2017), which is also used in the present work. Gamma tanycytes share every important characteristic of ependymal tanycytes, including morphology, ultrastructural features, and gene expression (Wittmann et al., 2017). The presence of γ tanycytes was also demonstrated in the mouse median eminence (Miranda-Angulo, Byerly, Mesa, Wang, & Blackshaw, 2014). Tanycyte-like cells in the arcuate nucleus parenchyma were described by Jourdon et al. (2016) as cells having tanycyte-like processes, elongated morphology and positive for genes characteristic of tanycytes including vimentin, nestin and Sox2. They demonstrated that at least some of these cells are Prss56-

expressing α2 tanycytes that migrated into the parenchyma (Jourdon et al., 2016). The same type of cell was also observed in the rat (Figure 3. in Millhouse, 1971), and the Mongolian gerbil (Figure 17. in Redecker, 1989b).

Results

Distribution and variability of Prss56 mRNA expression in tanycytes of adult rats

FISH for *Prss56* was performed on 4 groups of adult rats on a total of 22 animals; body weights and ages are included in Table 1. The number of *Prss56* mRNA-expressing tanycytes showed a striking variation among individual brains. Examples of high, intermediate and low *Prss56* expression throughout the rostro-caudal extent of the tanycyte region in separate brains are shown in Figs. 1 and 2. *Prss56* expression, as observed in brains with high *Prss56* levels, showed marked regional differences between tanycyte subpopulations. This was especially characteristic in the rostral half of the tanycyte region, where *Prss56* was prominently expressed in the α1 tanycyte area, as well as in the ventral portion of α2 tanycytes and β1 tanycytes, but conspicuously absent between these two locations (Fig. 1a, b). This gap, corresponding to the location of dorsal α2 tanycytes, disappeared caudally, beginning approximately at Bregma −3.2 mm, from which Prss56-expressing tanycytes were evenly distributed in the α1/2 and β1 tanycyte domains, to the caudal end of the ventricle (Fig. 2a, b). *Prss56* mRNA was virtually absent from β2 tanycytes in the floor of the ventricle, but was expressed in a subset of γ tanycytes (see definition in *Tanycyte Nomenclature)* in the median eminence, characteristically in those extending diagonally from the β1 domain (Fig. 1b3, Fig. 2b3), and occasionally in the infundibular stalk. In brains with intermediate *Prss56* levels, a reduced number of Prss56-expressing tanycytes was detected in all of these domains (Figs. 1c, 2c). In brains with low *Prss56* levels, the number of Prss56-expressing tanycytes was only a small fraction of those seen in “high *Prss56”* brains (Figs. 1d, e and 2d, e). This was especially prominent in the caudal half of the tanycyte region, where often just few β1 and γ tanycytes were *Prss56* positive in these brains (Fig. 2d2, e2). Low and high *Prss56* expression was observed in all four groups of rats, that is, among 8–10 weeks old males, females and 15-week-old males (Table 1). Repeated hybridization yielded the same labeling patterns in each brain, confirming that the observed variations were due to different *Prss56* mRNA levels in tanycytes.

Phenotypic characterization of Prss56-expressing cells along the third ventricle confirmed their identity as tanycytes. In the domain of α1 tanycytes, where the ependyma is 2–4 cell-layer thick, most Prss56-expressing cells were characteristically in the layer facing the parenchyma (Fig. 3), corresponding to the location of tanycytes in this zone (Altman & Bayer, 1978; Mathew, 2008; Perez-Martin et al., 2010). The vast majority of these *Prss56* cells expressed vimentin and GFAP (Fig. 3), and had the morphology of tanycytes, with basal processes extending into the parenchyma, and sometimes visible apical processes toward the ventricle, consistent with previous descriptions (Perez-Martin et al., 2010). In the α2 and β1 domains and the median eminence, *Prss56*-expressing cells also had the typical morphology of tanycytes, were positive for vimentin and often also for GFAP, although GFAP staining in the cell bodies of these subpopulations was lighter.

In addition to tanycytes, *Prss56* hybridization signal was also conspicuous in scattered cells in the arcuate and ventromedial nuclei, and in the pars tuberalis of the pituitary (see below). We observed some background-like labeling in neurons of the arcuate nucleus, localized typically over nuclei and not in the cytoplasm (data not shown). As this labeling did not appear in sections hybridized with the sense transcript, we are uncertain of its significance.

Prss56 expression inversely correlates with Pomc in adult rat tanycytes

The 22 adult rats used for this study were also used in our previous *Pomc* study (Wittmann et al., 2017), and it was immediately apparent that the brains with low *Prss56* expression had high *Pomc* levels in tanycytes (Fig. 4a, b), and vice versa (Fig. 4c, d; for more examples see b, d and e in Figs 1&2, and the corresponding *Pomc* images from the same brains in A, D and E, respectively, in Figs. 1&2 in Wittmann et al., 2017). To quantify this inverse relationship, we measured the areas covered by *Prss56* and *Pomc* ISH signals over the tanycyte region in each brain. A very strong inverse correlation was found between *Pomc* and *Prss56* expression in tanycytes, with correlation coefficient $r=-0.83$ ($p<0.0001$; $n=22$) (Fig. 4e). To describe in qualitative terms previously used to categorize tanycyte *Pomc* levels (Wittmann et al., 2017), all "high *Pomc*" brains had low *Prss56* levels, whereas all "low *Pomc*" brains had high *Prss56* levels (Fig. 4e). Of the five brains with intermediate *Pomc* levels, 3 had intermediate, 1 low and 1 high *Prss56* expression in tanycytes.

To determine whether individual tanycytes express both *Prss56* and *Pomc*, we performed dual-label ISH, using radioactive detection for *Prss56* and fluorescent detection for *Pomc* (Fig. 5). In general, *Prss56* and *Pomc* were expressed in distinct tanycytes, often interdigitating in the α2 and β1 domains, where both transcripts are expressed (Fig. 5b). In rare cases, however, both hybridization signals appeared to colocalize in the same tanycytes, as shown in a brain with intermediate *Pomc* and *Prss56* expression levels (Fig. 5b, c).

Prss56 mRNA expression in tanycytes of adolescent rats

We previously reported that *Pomc* expression in tanycytes was uniformly low among adolescent, postnatal 32-day-old male ($n=4$, body weight 80–93g) and female ($n=4$, 6781g) rats (Wittmann et al., 2017). In these same young animals, *Prss56* expression in tanycytes was uniformly high (Fig. 6). The basic distribution of *Prss56* was identical to that of adult "high *Prss56"* rats, but overall an even higher proportion of tanycytes expressed *Prss56*, including more γ tanycytes in the median eminence (Fig. 6a3).

Characteristics of parenchymal Prss56-expressing cells in rats

Scattered Prss56-expressing cells were observed in the hypothalamic parenchyma near the tanycyte region. The number of these cells correlated with *Prss56* expression in tanycytes ($r=0.61$, $p=0.0024$, $n=22$) and thus, on average, was lower in "low *Prss56*" than in "high *Prss56*" brains (Fig. 6g). To provide better characterization of these interesting cells, 10 brains were analyzed in greater detail (Groups 3&4 in Table 1). The number of parenchymal *Prss56* cells counted in every 12th 18μm-thick section ranged between 37 and 95 per brain (mean: 64.6 ± 6.5). Thus, we estimate the total number of these cells range between 300 and 900 per brain (37 or 95 ×12×0.76; 0.76 is the factor used to correct for profile overcounting). Except for rare cells in the ventral or caudal dorsomedial nucleus, parenchymal *Prss56* cells

were distributed in the ventromedial and arcuate nuclei in approximately equal numbers (Fig. 7, 8). In the rostro-caudal direction, their number sharply decreased toward the caudal end of the ventromedial nucleus (Fig. 7h).

Dual labeling with vimentin or GFAP clearly revealed that parenchymal *Prss56* cells were situated adjacent to the ventrolaterally arching trajectory of tanycyte processes arising from the third ventricle wall (Fig. 7, 8). In general, parenchymal *Prss56* cells had a size and shape (oval or elongated) similar to tanycytes, and frequently had tanycyte-like processes (Fig. 7, 8). The vast majority (91.8±1.5%; n=251 cells from 4 rats) were positive for vimentin (Fig. 7), although many were only lightly labeled, sometimes vimentin detectable only in their processes but not in the cell body. Most were also positive for GFAP (81.8±1.7%; n=309 cells from 4 rats) (Fig. 8), but they were always negative for the neuronal marker, Hu (data not shown). Thus, most parenchymal *Prss56*- expressing cells were tanycyte-like cells, homologous to those described by Jourdon et al. (2016) in $Prss56^{Cre/+},Rosa26^{tdTom/+}$ mice (see definition in *Tanycyte Nomenclature* above). Interestingly, parenchymal *Prss56* cells were often found in pairs, their cell bodies directly adjacent or making contact (Fig. 7, 8). In some cases, 3 to 6 cells were closely associated (Fig. 7b, e, f, 8c). The proportion of closely associated cells was estimated between 14–42% of all parenchymal *Prss56* cells (27.7 ± 3.1%, from 10 rats). Parenchymal tanycyte-like *Prss56* cells were uniformly numerous in adolescent rats (Fig. 6).

Ki-67 in rat tanycytes and parenchymal Prss56-expressing cells

To determine whether the variations in *Prss56* expression correlate with the proliferation activity of tanycytes and whether parenchymal Prss56-expressing cells are able to divide, we immunolabeled for the Ki-67 antigen, a cellular proliferation marker, in 6 male and 6 female adult rats (Groups 1&2 in Table 1). The number of Ki-67-positive cells in the tanycyte region and the surrounding hypothalamic parenchyma was highly variable (Fig. 9c) but did not correlate with *Prss56* or *Pomc* expression in tanycytes. Overall, fewer Ki- 67-positive cells were observed in females than in males in both the tanycyte region and the parenchyma (Fig. 9c). The validity of these differences in Ki-67 labeling was confirmed by a repeated Ki-67 immunostaining in the same brains (using a different protocol), which yielded the same patterns. It is noteworthy that in four brains, we observed a conspicuous concentration of Ki-67-positive cells in the ventricular wall (Fig. 9a, b), which appears to be identical to the group of proliferative cells visualized by 5- bromo-2'-deoxyuridine (BrdU) labeling in previous studies (Perez-Martin et al., 2010; Xu et al., 2005). This proliferative zone was approximately between Bregma −3.0 and −3.4 mm, in the α1 tanycyte domain. Ki-67 cells were positive for vimentin and positioned characteristically in the layer of tanycytes in this zone (Fig. 9b) (Altman & Bayer, 1978; Mathew, 2008; Perez-Martin et al., 2010). In the 3 male and 1 female brain, this proliferative zone contained from 11 to 25 Ki-67 cells per section, extending from 1 to 3 consecutive sections (each ~200μm away). Repeated Ki-67 immunostaining revealed the same concentration of Ki-67 cells in this zone in the same brains.

Few Prss56-expressing tanycytes were Ki-67 positive (Fig. 9 d-f, h): 4.5 ± 1.0 cells per brain (n=12 rats), a total of 52 cells that included tanycytes from each Prss56-expressing subtype

(α1, α2, β1 and γ). Parenchymal Prss56-expressing cells were occasionally Ki- 67 positive (Fig. 9f, g): a total of 7 such cells were found.

Prss56 expression in the pars tuberalis of the rat pituitary

Prss56 mRNA was expressed in the pars tuberalis of the pituitary that lies adjacent to the median eminence. The specificity of this hybridization signal was confirmed by the lack of signal in control hybridizations using the sense transcript (Fig. 10a, b). *Prss56* expression in the pars tuberalis was also highly variable among brains, but did not correlate with *Prss56* expression in tanycytes, or age/sex. Of the 22 adult rats, nine had very low expression, with fewer than 5 clearly labeled cells; nine had medium, with more labeled cells and cell clusters (seen on Fig. 1b2, e3); and four high, with intensely labeled cells and cell clusters. High levels of *Prss56* expression in the pars tuberalis were observed in brains with both low and high tanycyte *Prss56* levels in tanycytes. *Prss56* expression was generally more intense in t- he rostral pars tuberalis, anterior to Bregma - 3.2 mm. Dual FISH from three brains with high *Prss56* expression revealed that virtually all Prss56-expressing cells expressed *Tshb* mRNA (Fig. 10c-f). Conversely, almost all *Tshb* cells expressed *Prss56* mRNA rostrally (Fig. 10c, d), but this ratio decreased caudally, where a significant portion (≥50%) of *Tshb* cells was negative for *Prss56* hybridization signal (Fig. 10e, f). In adolescent rats, *Prss56* expression in the pars tuberalis was very low (<5 clearly labeled cells in each brain; Fig. 6).

Prss56 expression in the mouse hypothalamus

Prss56 expression was studied in the hypothalami of 10 adult mice: seven males (four of age postnatal day 53, body weight 22.1–24.9g, and three P65, 23–24.8g) and three females (P65, 17.3–18.9g). *Prss56* expression was consistently low in all 10 mice (Fig. 11). Only few labeled tanycytes were observed in each brain (27.5 ± 2.5; Fig. 11e), generally in a scattered distribution or loose groups. Fig. 11a and b show the distribution pattern in two brains. Most *Prss56* mRNA-expressing tanycytes belonged to the α2 or β1 subpopulation, but occasionally were α1 or γ tanycytes. We observed a case of *Prss56* expression in a tight group of approximately ten α2 tanycytes including one detached from the ependyma, toward the parenchyma (Fig. 11c), suggesting local activation of the *Prss56* gene and tanycyte translocation into the parenchyma (Jourdon et al., 2016). Of the parenchymal Prss56-expressing cells (3.4 ± 0.9, Fig. 11 e), all were observed in the arcuate nucleus or the retrochiasmatic area (Fig. 11a, b, d), except one in the ventromedial nucleus (Fig. 11b3). These cells were more frequent in rostral and mid levels of the arcuate nucleus (Fig. 11a, b), most positive for vimentin (76.5%, 26 of 34) (Fig. 11), and none expressed the neuronal protein, Hu (data not shown). As in rats, some of these cells were found in adjacent pairs (Fig. 11a, d) and distributed along the processes of tanycytes (Fig. 11d1). No hybridization signal was observed in the pars tuberalis in mice.

Prss56 expression in adolescent, postnatal 33-day-old male (n=4; BW 14.2–17.8g) and female (BW 13.5–14.3g) mice was similar to that seen in adults. The number of *Prss56*-expressing tanycytes and parenchymal cells was 39.1 ± 3.2 and 3.3 ±1.2, respectively, and all parenchymal Prss56-expressing cells were positive for vimentin.

Discussion

In the present study, we identified *Prss56* as a second gene with variable expression levels in tanycytes of adult rats that correlate inversely with tanycyte *Pomc* levels. There are only two plausible explanations for such variable expression: static expression that varies from animal to animal, or expression that oscillates in each animal. It is important to reiterate that the observed variations are not due to circadian rhythm, as rats with different expression levels were euthanized at the same time of the day. We also excluded an alternative explanation of age-related increase/decline in gene expression with a varied onset, by showing that high Pomc/low *Prss56* and low Pomc/high *Prss56* levels occur in two substantially different age groups, 8 and 15 week-old rats.

Based on the prevalence of periodic oscillatory gene expression in cells and tissues of various organisms (Eser et al., 2014; Hendriks, Gaidatzis, Aeschimann, & Grosshans, 2014; Imayoshi & Kageyama, 2014; Kageyama, Niwa, Isomura, Gonzalez, & Harima, 2012; Moreno-Risueno et al., 2010; Shimojo & Kageyama, 2016) we propose the working hypothesis that *Pomc* and *Prss56* expression oscillate in rat tanycytes, with alternating phases of high *Pomc*/low *Prss56* and low *Pomc*/high *Prss56* levels, while intermediate levels represent transitioning between these phases. Ultimately, unequivocal proof for this hypothesis will require transgenic rats in which a fluorescent transcriptional reporter protein is driven by the *Pomc* or *Prss56* promoter. Such a model will also allow determination of the temporal dynamics of the putative oscillatory cycles. Interestingly, periodic oscillatory gene expression is common during development in mammalian stem cells and neural progenitor cells (Imayoshi & Kageyama, 2014; Roese-Koerner, Stappert, & Brustle, 2017; Shimojo & Kageyama, 2016; Suzuki, Furusawa, & Kaneko, 2011; William et al., 2007), and tanycytes are now recognized as adult neural stem and progenitor cells because they can self-renew and also differentiate into neurons or astrocytes (Chaker et al., 2016; Haan et al., 2013; Lee et al., 2012; Robins et al., 2013; Xu et al., 2005). Thus, periodic gene expression in tanycytes may be a characteristic related specifically to their stem/progenitor cell properties, which is also supported by the fact that *Prss56* is specific to stem or progenitor cells in the brain, retina and skin (Gresset et al., 2015; Jourdon et al., 2016; Paylakhi et al., 2018).

Possible functional relationship between POMC and Prss56

This study revealed a strong, negative correlation between *Pomc* and *Prss56* expression in tanycytes, not only in adult, but also in adolescent rats in which uniformly high *Prss56* levels accompanied uniformly low *Pomc* expression (Wittmann et al., 2017). While correlation does not imply causation, it raises the possibility that POMC and Prss56 proteins may interact functionally, and one regulates the expression of the other. This possibility is supported by data that some periodically oscillating genes regulate others that oscillate out of phase with them (Bonev, Stanley, & Papalopulu, 2012; Imayoshi et al., 2013; Moreno-Risueno et al., 2010; Shimojo, Ohtsuka, & Kageyama, 2008; Uriu, 2016).

Since POMC is a secretory protein (Cawley et al., 2016), presumably it is also secreted by tanycytes. We hypothesize that it may have a paracrine and/or autocrine effects on tanycytes, similar to other secretory proteins synthesized by tanycytes such as ciliary neurotrophic factor (Kokoeva, Yin, & Flier, 2005; Severi et al., 2012; Severi et al., 2015). This hypothesis

raises the question as to what receptor/signaling pathway tanycyte-derived POMC may activate, as ACTH and α-MSH is absent or barely detectable in tanycytes, while the production of β-endorphin remains unclear (Wittmann et al., 2017). In addition, melanocortin or opioid receptors have not been identified in rat tanycytes (Abbadie, Pan, & Pasternak, 2000; Jegou, Boutelet, & Vaudry, 2000; Kishi et al., 2003; Mountjoy, Mortrud, Low, Simerly, & Cone, 1994; Roselli-Rehfuss et al., 1993; Xia & Wikberg, 1997). Thus, tanycytes may utilize N-terminal POMC (N-POMC) peptides for paracrine signaling, which we hypothesize would be advantageous to avoid interference with melanocortin signaling in the arcuate nucleus. Currently little is known about the biological effects of N-POMC peptides and their mechanism of action. In the adrenal cortex, they stimulate cell proliferation (Bicknell, 2016; Lotfi & de Mendonca, 2016), mediated by a locally expressed membrane-bound serine protease, adrenal secretory protease, which cleaves pro-γ-MSH, the large, inactive N-POMC fragment in the circulation (Eipper & Mains, 1978; Jackson, Salacinski, Hope, & Lowry, 1983), to a smaller fragment that has mitogenic effect (Bicknell, 2016; Bicknell et al., 2001). It is intriguing that Prss56 is similar to the adrenal secretory protease, also being a membrane-bound/secreted trypsin-like serine protease with trypsin-like activity (Nair et al., 2011). Since even a simple trypsin digestion of pro-γ-MSH produces peptides with mitogenic effect (Estivariz, Hope, McLean, & Lowry, 1980; Lotfi & de Mendonca, 2016), we hypothesize that Prss56, expressed on the cell membrane of tanycytes may cleave full-length POMC to smaller N-POMC peptides that may induce signal transduction in tanycytes.

That tanycytes release the POMC precursor is supported by earlier data that identified the full-size POMC precursor as the predominant form of POMC in the rat cerebrospinal fluid (in contrast to the hypothalamus, where it is α-MSH) (Pritchard et al., 2003). POMC released into the cerebrospinal fluid from β and ventral α2 tanycytes (Wittmann et al., 2017) would not only reach Prss56-expressing tanycytes in the same subpopulations, but also in the more distant α1 and dorsal α2 tanycyte domains. It is conceivable that increased N-POMC signaling may eventually lead to the downregulation of *Prss56,* thus driving its oscillations in a synchronized manner across different subpopulations. Further studies will be necessary to determine whether POMC is a substrate of Prss56 and also regulates its expression, or alternatively, the oscillations of these genes are driven independently of one another and only indirectly related.

Prss56 as a possible marker for migrating and differentiating cells of tanycyte origin

Jourdon et al. (2016) demonstrated that *Prss56* is expressed specifically in neural stem/progenitor cells in the adult and embryonic mouse brain, and that reporter expression in $Prss56^{Cre/}$,$Rosa26^{tdTom+}$ mice labels the successive steps of neurogenesis in adult neurogenic zones. In the hypothalamus, tdTomato appears in tanycytes at an early postnatal age, but by postnatal day 90, the reporter also labels a substantial number of neurons in the arcuate nucleus (Jourdon et al., 2016). Since neurons do not express *Prss56* (Jourdon et al., 2016), which we confirmed in the present study, the distribution of tdTomato suggests that Prss56-expressing tanycytes, or at least a portion of them, are neurogenic during young postnatal and/or early adult life. Jourdon et al. (2016) also demonstrated that reporter positive tanycyte-like cells in the arcuate nucleus parenchyma arise from α2 tanycytes, and

are potentially the precursors that will differentiate into neurons. In light of these data, the very limited number of Prss56-expressing cells observed in adult mice, with the number of tanycytes apparently fewer than reporter-positive tanycytes in Jourdon's study (2016), suggests that *Prss56* is expressed transiently, only by few tanycytes at any given time, some of which migrate into the parenchyma.

Parenchymal Prss56-expressing cells in both rats and mice are distributed in close apposition along the trajectory of tanycyte processes that originate from cell bodies in the wall of the third ventricle, suggesting that tanycyte processes may guide their movement within the parenchyma. Previous studies also noted the juxtaposition of tanycyte processes and tanycyte-derived cells (Robins et al., 2013; Xu et al., 2005). We hypothesize that Prss56, being a membrane-bound or secreted protease, may facilitate the migration of these cells by degrading extracellular matrix proteins and/or disrupting cell adhesion molecules on the cell surface (Nair et al., 2011; Paylakhi et al., 2018). It is also of interest that parenchymal *Prss56*-expressing cells were often found as adjacent pairs, or sometimes as multiple adjacent cells, suggesting that two or more Prss56-expressing tanycytes migrate together into the parenchyma and/or some of these cells divide while in the parenchyma. Indeed, we found a few cases of Ki-67-positive parenchymal *Prss56*- expressing cells in rats. While most parenchymal *Prss56*-expressing cells were tanycyte-like cells, a minority in both rats and mice were negative for vimentin, raising the possibility that they degraded vimentin and in the process of differentiating into neurons or astrocytes (Chaker et al., 2016; Jourdon et al., 2016).

Conclusions

We conclude that *Prss56* and *Pomc* are two genes that are expressed variably in an inverse manner in rat tanycytes, suggesting the existence of periodically oscillating gene expression in these cells. Further studies are required to identify the full complement of similarly expressed genes in tanycytes, and to uncover the functional significance of this phenomenon. In addition, we demonstrate that *Prss56* expression identifies a population of tanycyte-like cells in the hypothalamic parenchyma that were previously reported to have neurogenic potential (Jourdon et al., 2016), and may serve as a marker for migrating and differentiating cells of tanycyte origin.

Acknowledgments:

This work was supported by NIH grant R21AG050663 and a grant from the Dr. Gerald J. and Dorothy R. Friedman New York Foundation for Medical Research.

References

Abbadie C, Pan YX, & Pasternak GW (2000). Differential distribution in rat brain of mu opioid receptor carboxy terminal splice variants MOR-1C-like and MOR-1- like immunoreactivity: evidence for region-specific processing. J Comp Neurol, 419(2), 244–256. doi:10.1002/(SICI)1096-9861(20000403)419:2<244::AID-CNE8>3.0.CO;2-R [pii] [PubMed: 10723002]

Akmayev IG, & Fidelina OV (1976). Morphological aspects of the hypothalamic-hypophyseal system. VI. The tanycytes: their relation to the sexual differentiation of the hypothalamus. An enzyme-histochemical study. Cell Tissue Res, 173(3), 407–416. [PubMed: 991250]

Akmayev IG, Fidelina OV, Kabolova ZA, Popov AP, & Schitkova TA (1973). Morphological aspects of the hypothalamic-hypophyseal system. IV. Medial basal hypothalamus. An experimental morphological study. Z Zellforsch Mikrosk Anat, 137(4), 493–512. [PubMed: 4348309]

Altman J, & Bayer SA (1978). Development of the diencephalon in the rat. III. Ontogeny of the specialized ventricular linings of the hypothalamic third ventricle. J Comp Neurol, 182(4 Pt 2), 995–1015. [PubMed: 730854]

Baubet V, Fevre-Montange M, Gay N, Debilly G, Bobillier P, & Cespuglio R (1994). Effects of an acute immobilization stress upon proopiomelanocortin (POMC) mRNA levels in the mediobasal hypothalamus: a quantitative in situ hybridization study. Brain Res Mol Brain Res, 26(1–2), 163–168. [PubMed: 7854043]

Bicknell AB (2016). 60 YEARS OF POMC: N-terminal POMC peptides and adrenal growth. J Mol Endocrinol, 56(4), T39–48. doi:JME-15–0269 [pii] 10.1530/JME-15-0269 [PubMed: 26759392]

Bicknell AB, Lomthaisong K, Woods RJ, Hutchinson EG, Bennett HP, Gladwell RT (2001). Characterization of a serine protease that cleaves progamma-melanotropin at the adrenal to stimulate growth. Cell, 105(7), 903–912. doi:S0092–8674(01)00403–2 [pii] [PubMed: 11439186]

Bitsch P, & Schiebler TH (1979). [Postnatal development of the median eminence in the rat]. Z Mikrosk Anat Forsch, 93(1), 1–20. [PubMed: 473854]

Bonev B, Stanley P, & Papalopulu N (2012). MicroRNA-9 Modulates Hes1 ultradian oscillations by forming a double-negative feedback loop. Cell Rep, 2(1), 10–18. doi:S2211–1247(12)00142–8 [pii] 10.1016/j.celrep.2012.05.017 [PubMed: 22840391]

Cawley NX, Li Z, & Loh YP (2016). 60 YEARS OF POMC: Biosynthesis, trafficking, and secretion of pro-opiomelanocortin-derived peptides. J Mol Endocrinol, 56(4), T77–97. doi:JME-15–0323 [pii] 10.1530/JME-15-0323 [PubMed: 26880796]

Chaker Z, George C, Petrovska M, Caron JB, Lacube P, Caille I (2016). Hypothalamic neurogenesis persists in the aging brain and is controlled by energy-sensing IGF-I pathway. Neurobiol Aging, 41, 64–72. doi:S0197– 4580(16)00151–2 [pii] 10.1016/j.neurobiolaging.2016.02.008 [PubMed: 27103519]

Chauvet N, Privat A, & Alonso G (1996). Aged median eminence glial cell cultures promote survival and neurite outgrowth of cocultured neurons. Glia, 18(3), 211–223. doi:10.1002/(SICI)1098-1136(1996n)18:3<2n::AID-GLIA5>3.0.CO;2-1 [Pii] 10.1002/(SICI)1098-n36(1996n)18:3<211::AID-GLIA5>3.0.CO;2–1 [PubMed: 8915653]

Eipper BA, & Mains RE (1978). Existence of a common precursor to ACTH and endorphin in the anterior and intermediate lobes of the rat pituitary. J Supramol Struct, 8(3), 247–262. doi:10.1002/jss.400080304 [PubMed: 82677]

Eser P, Demel C, Maier KC, Schwalb B, Pirkl N, Martin DE (2014). Periodic mRNA synthesis and degradation co-operate during cell cycle gene expression. Mol Syst Biol, 10, 717. doi:10/1/717 [pii] 10.1002/msb.134886 [PubMed: 24489117]

Estivariz FE, Hope J, McLean C, & Lowry PJ (1980). Purification and characterization of a gamma-melanotropin precursor from frozen human pituitary glands. Biochem J, 191(1), 125–132. [PubMed: 7470089]

Gresset A, Coulpier F, Gerschenfeld G, Jourdon A, Matesic G, Richard L (2015). Boundary Caps Give Rise to Neurogenic Stem Cells and Terminal Glia in the Skin. Stem Cell Reports, 5(2), 278–290. doi:S2213–6711(15)00186–1 [pii] 10.1016/j.stemcr.2015.06.005 [PubMed: 26212662]

Guillery RW (2002). On counting and counting errors. J Comp Neurol, 447(1), 1–7. doi:10.1002/cne.10221 [PubMed: 11967890]

Haan N, Goodman T, Najdi-Samiei A, Stratford CM, Rice R, El Agha E (2013). Fgf10-expressing tanycytes add new neurons to the appetite/energy-balance regulating centers of the postnatal and adult hypothalamus. J Neurosci, 33(14), 6170–6180. doi:33/14/6170 [pii] 10.1523/JNEUROSCI.2437-12.2013 [PubMed: 23554498]

Hendriks GJ, Gaidatzis D, Aeschimann F, & Grosshans H (2014). Extensive oscillatory gene expression during C. elegans larval development. Mol Cell, 53(3), 380–392. doi:S1097–2765(13)00903–9 [pii] 10.1016/j.molcel.2013.12.013 [PubMed: 24440504]

Hokfelt T, Foster G, Schultzberg M, Meister B, Schalling M, Goldstein M (1988). DARPP-32 as a marker for D-1 dopaminoceptive cells in the rat brain: prenatal development and presence in glial

elements (tanycytes) in the basal hypothalamus. Adv Exp Med Biol, 235, 65–82. [PubMed: 2976255]

Imayoshi I, Isomura A, Harima Y, Kawaguchi K, Kori H, Miyachi H (2013).Oscillatory control of factors determining multipotency and fate in mouse neural progenitors. Science, 342(6163), 1203–1208. doi:science.1242366 [pii] 10.1126/science.1242366 [PubMed: 24179156]

Imayoshi I, & Kageyama R (2014). Oscillatory control of bHLH factors in neural progenitors. Trends Neurosci, 37(10), 531–538. doi:S0166–2236(14)00122–2 [pii] 10.1016/j.tins.2014.07.006 [PubMed: 25149265]

Jackson S, Salacinski P, Hope J, & Lowry PJ (1983). An investigation of N-terminal pro-opiocortin peptides in the rat pituitary. Peptides, 4(4), 431–438. doi:0196–9781(83)90045–1 [pii] [PubMed: 6316293]

Jegou S, Boutelet I, & Vaudry H (2000). Melanocortin-3 receptor mRNA expression in pro-opiomelanocortin neurones of the rat arcuate nucleus. J Neuroendocrinol, 12(6), 501–505. doi:jne477 [pii] [PubMed: 10844578]

Jourdon A, Gresset A, Spassky N, Charnay P, Topilko P, & Santos R (2016). Prss56, a novel marker of adult neurogenesis in the mouse brain. Brain Struct Funct, 221(9), 4411–4427. doi:10.1007/s00429-015-1171-z [pii] [PubMed: 26701169]

Kageyama R, Niwa Y, Isomura A, Gonzalez A, & Harima Y (2012). Oscillatory gene expression and somitogenesis. Wiley Interdiscip Rev Dev Biol, 1(5), 629–641. doi:10.1002/wdev.46 [PubMed: 23799565]

Kawakami S (2000). Glial and neuronal localization of ionotropic glutamate receptor subunit-immunoreactivities in the median eminence of female rats: GluR2/3 and GluR6/7 colocalize with vimentin, not with glial fibrillary acidic protein (GFAP). Brain Res, 858(1), 198–204. doi:S0006899300019806 [pii] [PubMed: 10700615]

Kishi T, Aschkenasi CJ, Lee CE, Mountjoy KG, Saper CB, & Elmquist JK (2003). Expression of melanocortin 4 receptor mRNA in the central nervous system of the rat. J Comp Neurol, 457(3), 213–235. doi:10.1002/cne.10454 [PubMed: 12541307]

Kokoeva MV, Yin H, & Flier JS (2005). Neurogenesis in the hypothalamus of adult mice: potential role in energy balance. Science, 310(5748), 679–683. doi:310/5748/679 [pii] 10.1126/science.1115360 [PubMed: 16254185]

Larsen PJ, & Mau SE (1994). Effect of acute stress on the expression of hypothalamic messenger ribonucleic acids encoding the endogenous opioid precursors preproenkephalin A and proopiomelanocortin. Peptides, 15(5), 783–790. [PubMed: 7984495]

Lee DA, Bedont JL, Pak T, Wang H, Song J, Miranda-Angulo A (2012). Tanycytes of the hypothalamic median eminence form a diet-responsive neurogenic niche. Nat Neurosci, 15(5), 700–702. doi:nn.3079 [pii] 10.1038/nn.3079 [PubMed: 22446882]

Lotfi CF, & de Mendonca PO (2016). Comparative Effect of ACTH and Related Peptides on Proliferation and Growth of Rat Adrenal Gland. Front Endocrinol (Lausanne), 7, 39. doi:10.3389/fendo.2016.00039 [PubMed: 27242663]

Lu XY, Shieh KR, Kabbaj M, Barsh GS, Akil H, & Watson SJ (2002). Diurnal rhythm of agouti-related protein and its relation to corticosterone and food intake. Endocrinology, 143(10), 3905–3915. doi:10.1210/en.2002-220150 [PubMed: 12239102]

Mathew TC (2008). Regional analysis of the ependyma of the third ventricle of rat by light and electron microscopy. Anat Histol Embryol, 37(1), 9–18. doi:AHE786 [pii] 10.1111/j.1439-0264.2007.00786.x [PubMed: 18197894]

Meister B, Hokfelt T, Tsuruo Y, Hemmings H, Ouimet C, Greengard P (1988). DARPP-32, a dopamine- and cyclic AMP-regulated phosphoprotein in tanycytes of the mediobasal hypothalamus: distribution and relation to dopamine and luteinizing hormone-releasing hormone neurons and other glial elements. Neuroscience, 27(2), 607–622. doi:0306–4522(88)90292–8 [pii] [PubMed: 2905789]

Millhouse OE (1971). A Golgi study of third ventricle tanycytes in the adult rodent brain. Z Zellforsch Mikrosk Anat, 121(1), 1–13. [PubMed: 5112429]

Miranda-Angulo AL, Byerly MS, Mesa J, Wang H, & Blackshaw S (2014). Rax regulates hypothalamic tanycyte differentiation and barrier function in mice. J Comp Neurol, 522(4), 876–899. doi:10.1002/cne.23451 [PubMed: 23939786]

Moreno-Risueno MA, Van Norman JM, Moreno A, Zhang J, Ahnert SE, & Benfey PN (2010). Oscillating gene expression determines competence for periodic Arabidopsis root branching. Science, 329(5997), 1306–1311. doi:329/5997/1306 [pii] 10.1126/science.1191937 [PubMed: 20829477]

Mountjoy KG, Mortrud MT, Low MJ, Simerly RB, & Cone RD (1994). Localization of the melanocortin-4 receptor (MC4-R) in neuroendocrine and autonomic control circuits in the brain. Mol Endocrinol, 8(10), 1298–1308. doi:10.1210/mend.8.10.7854347 [PubMed: 7854347]

Nair KS, Hmani-Aifa M, Ali Z, Kearney AL, Ben Salem S, Macalinao DG (2011). Alteration of the serine protease PRSS56 causes angle-closure glaucoma in mice and posterior microphthalmia in humans and mice. Nat Genet, 43(6), 579–584. doi:ng.813 [pii] 10.1038/ng.813 [PubMed: 21532570]

Paylakhi S, Labelle-Dumais C, Tolman NG, Sellarole MA, Seymens Y, Saunders J (2018). Muller glia-derived PRSS56 is required to sustain ocular axial growth and prevent refractive error. PLoS Genet, 14(3), e1007244. doi :10.1371/journal.pgen.1007244 PGENETICS-D-17–01368 [pii] [PubMed: 29529029]

Perez-Martin M, Cifuentes M, Grondona JM, Lopez-Avalos MD, Gomez-Pinedo U, Garcia-Verdugo JM (2010). IGF-I stimulates neurogenesis in the hypothalamus of adult rats. Eur J Neurosci, 31(9), 1533–1548. doi:EJN7220 [pii] 10.1111/j.1460-9568.2010.07220.x [PubMed: 20525067]

Pritchard LE, Oliver RL, McLoughlin JD, Birtles S, Lawrence CB, Turnbull AV (2003). Proopiomelanocortin-derived peptides in rat cerebrospinal fluid and hypothalamic extracts: evidence that secretion is regulated with respect to energy balance. Endocrinology, 144(3), 760–766. doi:10.1210/en.2002-220866 [PubMed: 12586751]

Redecker P (1989a). Immunogold electron microscopic localization of glial fibrillary acidic protein (GFAP) in neurohypophyseal pituicytes and tanycytes of the Mongolian gerbil (Meriones unguiculatus). Histochemistry, 91(4), 333–337. [PubMed: 2732098]

Redecker P (1989b). Postnatal development of glial fibrillary acidic protein (GFAP) immunoreactivity in pituicytes and tanycytes of the Mongolian gerbil (Meriones unguiculatus). Histochemistry, 91(6), 507–515. [PubMed: 2670844]

Redecker P (1990). The glial architecture of the median eminence of the Mongolian gerbil (Meriones unguiculatus); a study of glial fibrillary acidic protein (GFAP) immunoreactivity in semithin sections. Acta Histochem, 88(2), 139–147. doi:S0065-1281(11)80126-1 [pii] 10.1016/S0065-1281(11)80126-1 [PubMed: 1699378]

Robins SC, Stewart I, McNay DE, Taylor V, Giachino C, Goetz M (2013). alpha-Tanycytes of the adult hypothalamic third ventricle include distinct populations of FGF-responsive neural progenitors. Nat Commun, 4, 2049. doi:ncomms3049 [pii] 10.1038/ncomms3049 [PubMed: 23804023]

Rodriguez EM, Gonzalez CB, & Delannoy L (1979). Cellular organization of the lateral and postinfundibular regions of the median eminence in the rat. Cell Tissue Res, 201(3), 377–408. [PubMed: 389426]

Roese-Koerner B, Stappert L, & Brustle O (2017). Notch/Hes signaling and miR-9 engage in complex feedback interactions controlling neural progenitor cell proliferation and differentiation. Neurogenesis (Austin), 4(1), e1313647. doi:10.1080/23262133.2017.1313647 [pii] [PubMed: 28573150]

Roselli-Rehfuss L, Mountjoy KG, Robbins LS, Mortrud MT, Low MJ, Tatro JB (1993). Identification of a receptor for gamma melanotropin and other proopiomelanocortin peptides in the hypothalamus and limbic system. Proc Natl Acad Sci U S A, 90(19), 8856–8860. [PubMed: 8415620]

Ross AW, Johnson CE, Bell LM, Reilly L, Duncan JS, Barrett P (2009).Divergent regulation of hypothalamic neuropeptide Y and agouti-related protein by photoperiod in F344 rats with differential food intake and growth. J Neuroendocrinol, 21(7), 610–619. doi:JNE1878 [pii] 10.1111/j.1365-2826.2009.01878.x [PubMed: 19490367]

Ross AW, Russell L, Helfer G, Thomson LM, Dalby MJ, & Morgan PJ(2015). Photoperiod regulates lean mass accretion, but not adiposity, in growing F344 rats fed a high fat diet. PLoS One, 10(3), e0119763. doi:10.1371/journal.pone.0119763 PONE-D-14–43404 [pii] [PubMed: 25789758]

Rutzel H, & Schiebler TH (1980). Prenatal and early postnatal development of the glial cells in the median eminence of the rat. Cell Tissue Res, 211(1), 117–137. [PubMed: 7407881]

Schindelin J, Arganda-Carreras I, Frise E, Kaynig V, Longair M, Pietzsch T (2012). Fiji: an open-source platform for biological-image analysis. Nat Methods, 9(7), 676–682. doi:nmeth.2019 [pii] 10.1038/nmeth.2019 [PubMed: 22743772]

Schneider CA, Rasband WS, & Eliceiri KW (2012). NIH Image to ImageJ: 25 years of image analysis. Nat Methods, 9(7), 671–675. [PubMed: 22930834]

Scholzen T, & Gerdes J (2000). The Ki-67 protein: from the known and the unknown.J Cell Physiol, 182(3), 311–322. doi:10.1002/(SICI)1097-4652(200003)182:3<311::AID-JCP1>3.0.CO;2-9 [pii] [PubMed: 10653597]

Sergeyev VG, Vegeyeva OA, & Akmayev IG (2011). Effect of intraperitoneal administration of bacterial lipopolysaccharide on synthesis of pro-opiomelanocortin mRNA in rat tanycytes. Bull Exp Biol Med, 150(4), 443–445. [PubMed: 22268039]

Severi I, Carradori MR, Lorenzi T, Amici A, Cinti S, & Giordano A (2012). Constitutive expression of ciliary neurotrophic factor in mouse hypothalamus. J Anat, 220(6), 622–631. doi:10.1111/j.1469-7580.2012.01498.x [PubMed: 22458546]

Severi I, Senzacqua M, Mondini E, Fazioli F, Cinti S, & Giordano A (2015). Activation of transcription factors STAT1 and STAT5 in the mouse median eminence after systemic ciliary neurotrophic factor administration. Brain Res, 1622, 217–229. doi:S0006–8993(15)00499–0 [pii] 10.1016/j.brainres.2015.06.028 [PubMed: 26133794]

Shimojo H, & Kageyama R (2016). Oscillatory control of Delta-like1 in somitogenesis and neurogenesis: A unified model for different oscillatory dynamics. Semin Cell Dev Biol, 49, 76–82. doi:S1084–9521(16)30017–9 [pii] 10.1016/j.semcdb.2016.01.017 [PubMed: 26818178]

Shimojo H, Ohtsuka T, & Kageyama R (2008). Oscillations in notch signaling regulate maintenance of neural progenitors. Neuron, 58(1), 52–64. doi:S0896– 6273(08)00166–9 [pii] 10.1016/j.neuron.2008.02.014 [PubMed: 18400163]

Suzuki N, Furusawa C, & Kaneko K (2011). Oscillatory protein expression dynamics endows stem cells with robust differentiation potential. PLoS One, 6(11), e27232. doi:10.1371/journal.pone.0027232 PONE-D-11–15659 [pii] [PubMed: 22073296]

Uriu K (2016). Genetic oscillators in development. Dev Growth Differ, 58(1), 16–30. doi:10.1111/dgd.12262 [PubMed: 26753997]

Willesen MG, Kristensen P, & Romer J (1999). Co-localization of growth hormone secretagogue receptor and NPY mRNA in the arcuate nucleus of the rat. Neuroendocrinology, 70(5), 306–316. doi:nen70306 [pii] [PubMed: 10567856]

William DA, Saitta B, Gibson JD, Traas J, Markov V, Gonzalez DM (2007). Identification of oscillatory genes in somitogenesis from functional genomic analysis of a human mesenchymal stem cell model. Dev Biol, 305(1), 172–186. doi :S0012–1606(07)00101–7 [pii] 10.1016/j.ydbio.2007.02.007 [PubMed: 17362910]

Wittkowski W (1980). Glia der Neurohypophyse In Oksche A (Ed.), Handbuch der mikroskopischen Anatomie des Menschen (Vol. 4/10, pp. 667–756). Berlin, Heidelberg, New York: Springer.

Wittkowski W (1998). Tanycytes and pituicytes: morphological and functional aspects of neuroglial interaction. Microsc Res Tech, 41(1), 29–42. doi:10.1002/(SICI)1097-0029(19980401)41:1<29::AID-JEMT4>3.0.CO;2-P [pii] [PubMed: 9550135]

Wittmann G, Farkas E, Szilvasy-Szabo A, Gereben B, Fekete C, & Lechan RM (2017). Variable proopiomelanocortin expression in tanycytes of the adult rat hypothalamus and pituitary stalk. J Comp Neurol, 525(3), 411–441. doi:10.1002/cne.24090 [PubMed: 27503597]

Wittmann G, Hrabovszky E, & Lechan RM (2013). Distinct glutamatergic and GABAergic subsets of hypothalamic pro-opiomelanocortin neurons revealed by in situ hybridization in male rats and mice. J Comp Neurol, 521(14), 3287–3302. doi:10.1002/cne.23350 [PubMed: 23640796]

Wittmann G, Mohacsik P, Balkhi MY, Gereben B, & Lechan RM (2015).Endotoxin-induced inflammation down-regulates L-type amino acid transporter 1 (LAT1) expression at the blood-

brain barrier of male rats and mice. Fluids Barriers CNS, 12, 21. doi:10.1186/s12987-015-0016-8 [pii] [PubMed: 26337286]

Wittmann G, Szabon J, Mohacsik P, Nouriel SS, Gereben B, Fekete C (2015). Parallel regulation of thyroid hormone transporters OATP1c1 and MCT8 during and after endotoxemia at the blood-brain barrier of male rodents. Endocrinology, 156(4), 1552–1564. doi:10.1210/en.2014-1830 [PubMed: 25594699]

Xia Y, & Wikberg JE (1997). Postnatal expression of melanocortin-3 receptor in rat diencephalon and mesencephalon. Neuropharmacology, 36(2), 217–224. doi:S0028390896001517 [pii] [PubMed: 9144659]

Xu Y, Tamamaki N, Noda T, Kimura K, Itokazu Y, Matsumoto N (2005).Neurogenesis in the ependymal layer of the adult rat 3rd ventricle. Exp Neurol, 192(2), 251–264. doi:S0014–4886(04)00508–4 [pii] 10.1016/j.expneurol.2004.12.021 [PubMed: 15755543]

Zaborszky L, & Schiebler TH (1978). [Glia of median eminence. Electron microscopic studies of normal, adrenalectomized and castrated rats]. Z Mikrosk Anat Forsch, 92(4), 781–799. [PubMed: 749399]

Zoli M, Ferraguti F, Frasoldati A, Biagini G, & Agnati LF (1995). Age-related alterations in tanycytes of the mediobasal hypothalamus of the male rat. Neurobiol Aging, 16(1), 77–83. doi: 0197458095800100 [pii] [PubMed: 7723939]

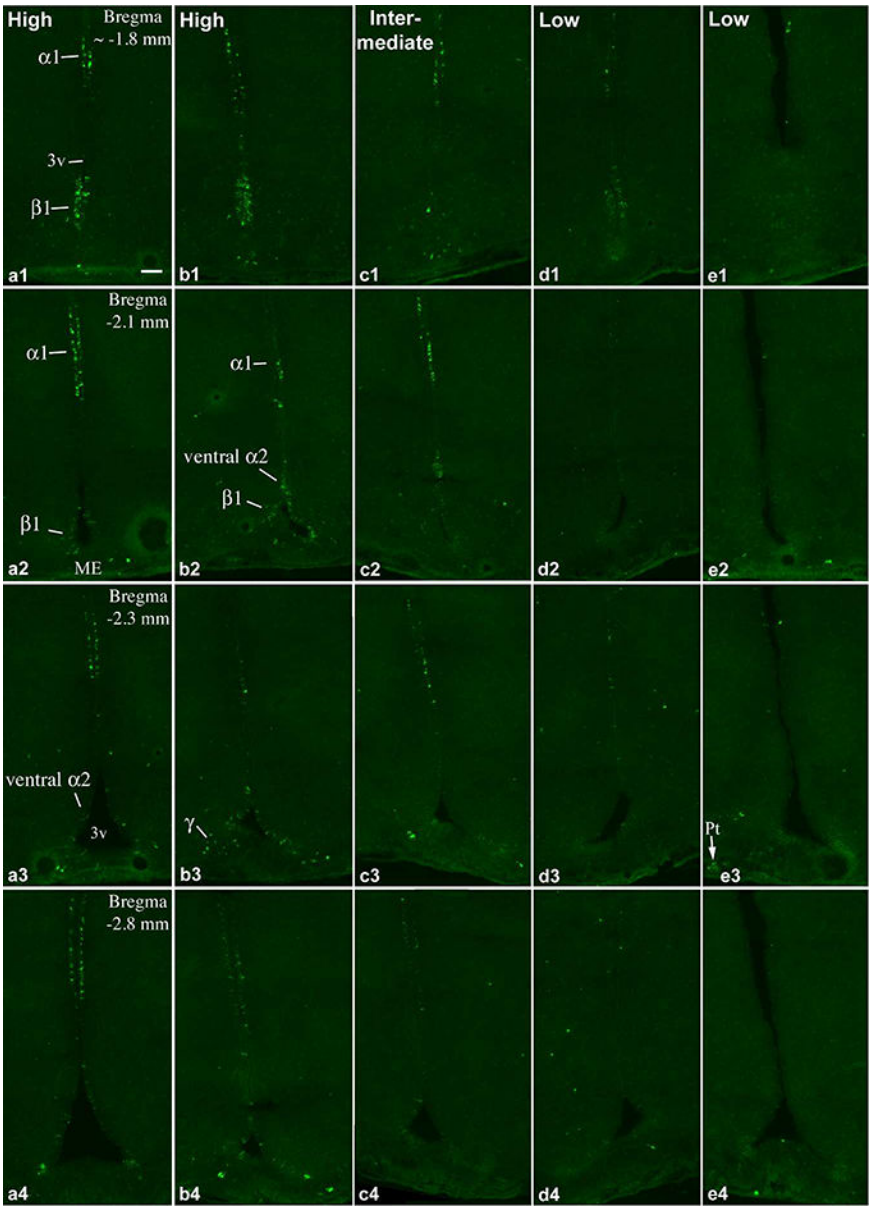

Figure 1.

FISH demonstrates *Prss56* mRNA-expressing cells in the rostral part of the tanycyte region in 5 adult rats with different expression levels. (a, b) High, (c) intermediate, (d, e) and low *Prss56* mRNA levels in tanycytes. a, c and e are female, b and d are male rats, between 8–10 weeks of age. The caudal tanycyte regions from the same brains are shown in Fig. 2. *Pomc* expression in brains b, d and e, are shown in Wittmann et al. (2017) in Figs. 1 and 2 in A, D and E, respectively. Tanycyte subtypes that express *Prss56* (α1, α2, β1 and γ) are indicated on a1-a3, b2, b3. Hybridization signal in the pars tuberalis (Pt) is indicated on e3. 3v, third ventricle; ME, median eminence. Scale bar: 100μm.

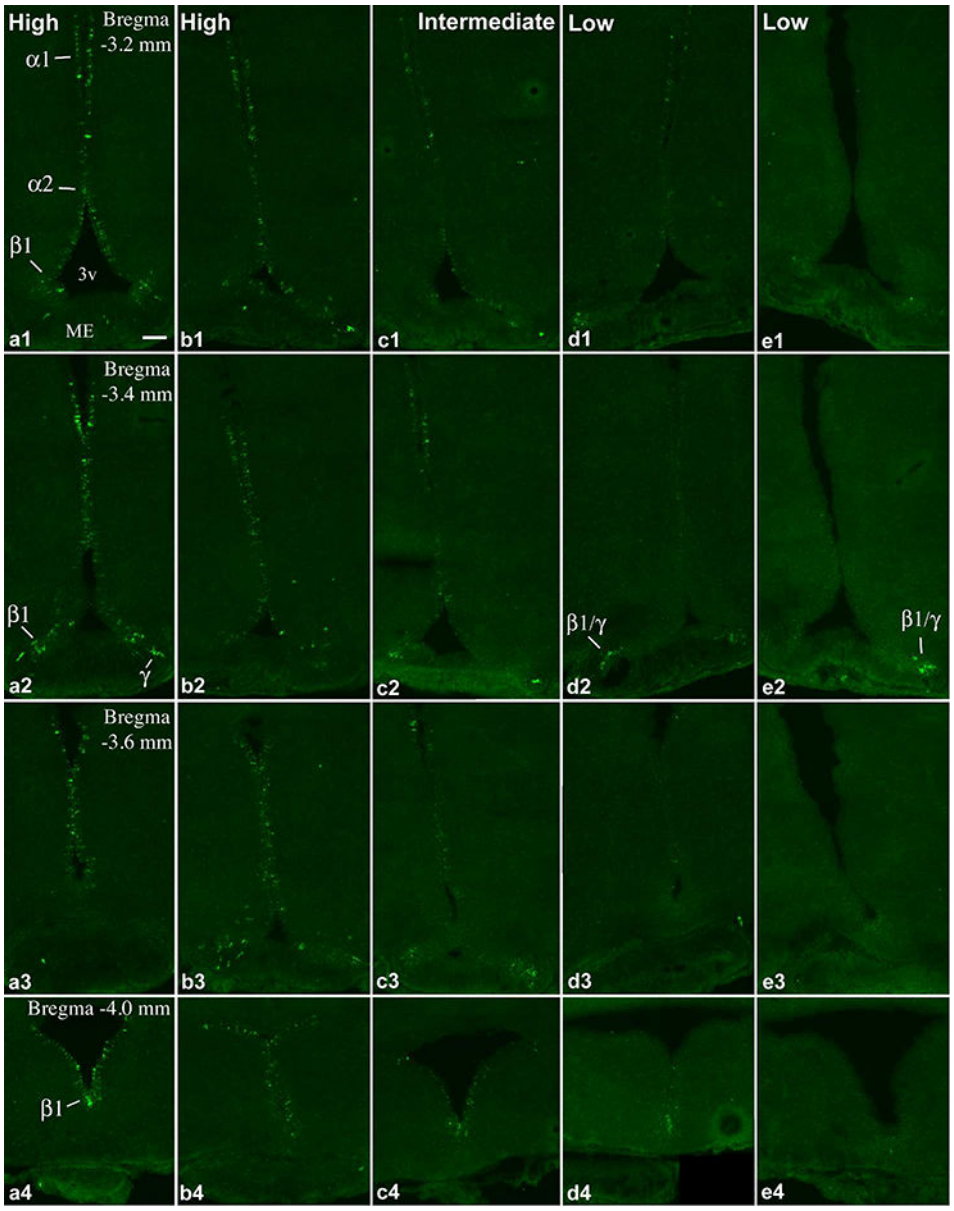

Figure 2.

Continuation of Figure 1. FISH demonstrates *Prss56* mRNA-expressing cells in the caudal part of the tanycyte region in 5 adult rats with different expression levels. (a, b) High, (c) intermediate, (d, e) and low *Prss56* mRNA levels in tanycytes. *Pomc* expression in brains b, d and e, are shown in A, D and E, respectively, of Figs. 1 and 2 in Wittmann et al. (2017). Tanycyte subtypes (α1, α2, β1 and γ) that express *Prss56* are indicated on a1, a2, a4, d2, e2. 3v, third ventricle; ME, median eminence. Scale bar: 100μm.

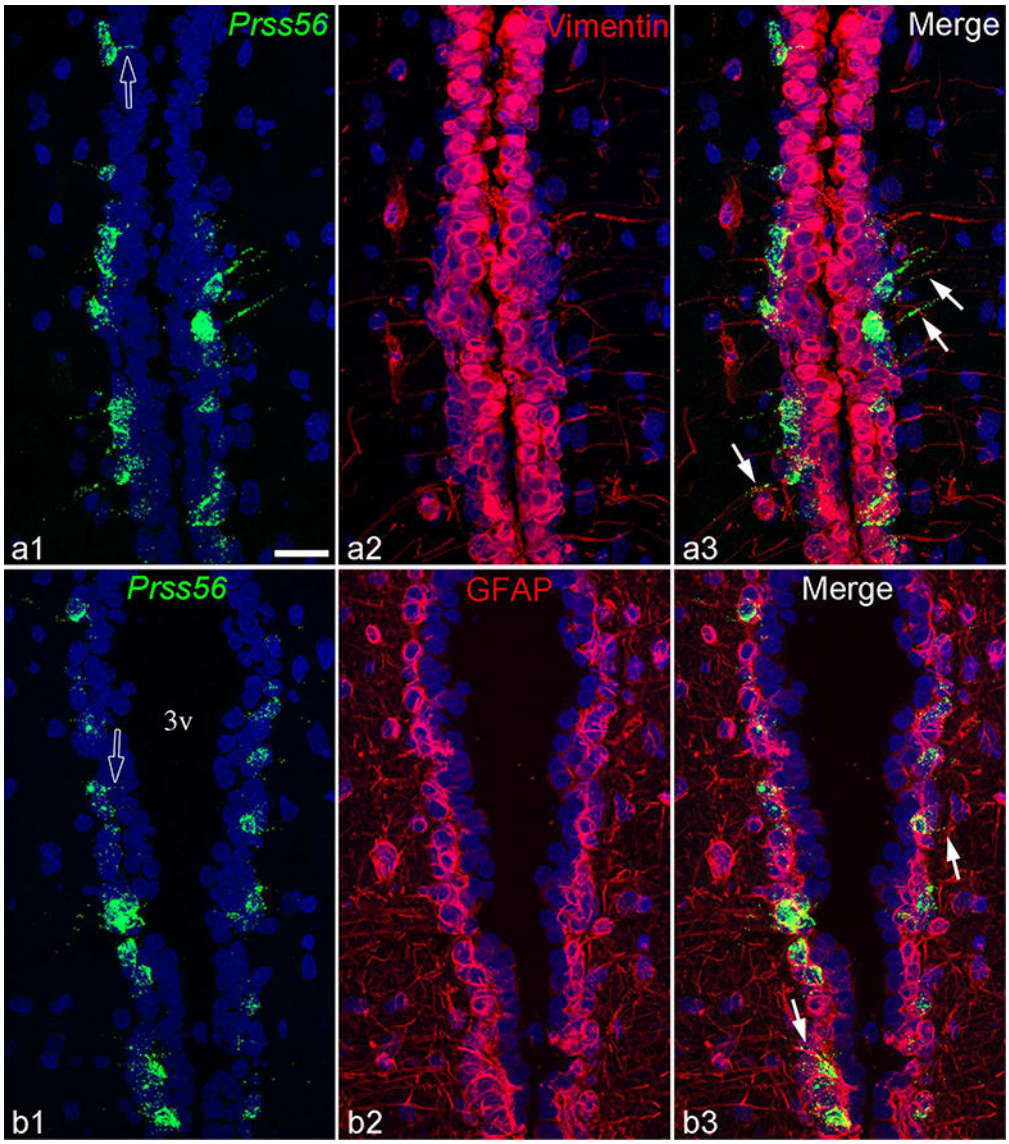

Figure 3.

Z-projections of confocal images demonstrate that Prss56-expressing tanycytes in the α1 tanycyte subpopulation express both vimentin (a1-a3) and GFAP (b1-b3). Open arrows in a1 and b1 indicate *Prss56* positive apical tanycyte processes projecting toward the ventricle; arrows in cl or c3 point to basal tanycyte processes that contain *Prss56* mRNA and vimentin or GFAP, respectively. 3v, third ventricle. Scale bar: 25μm.

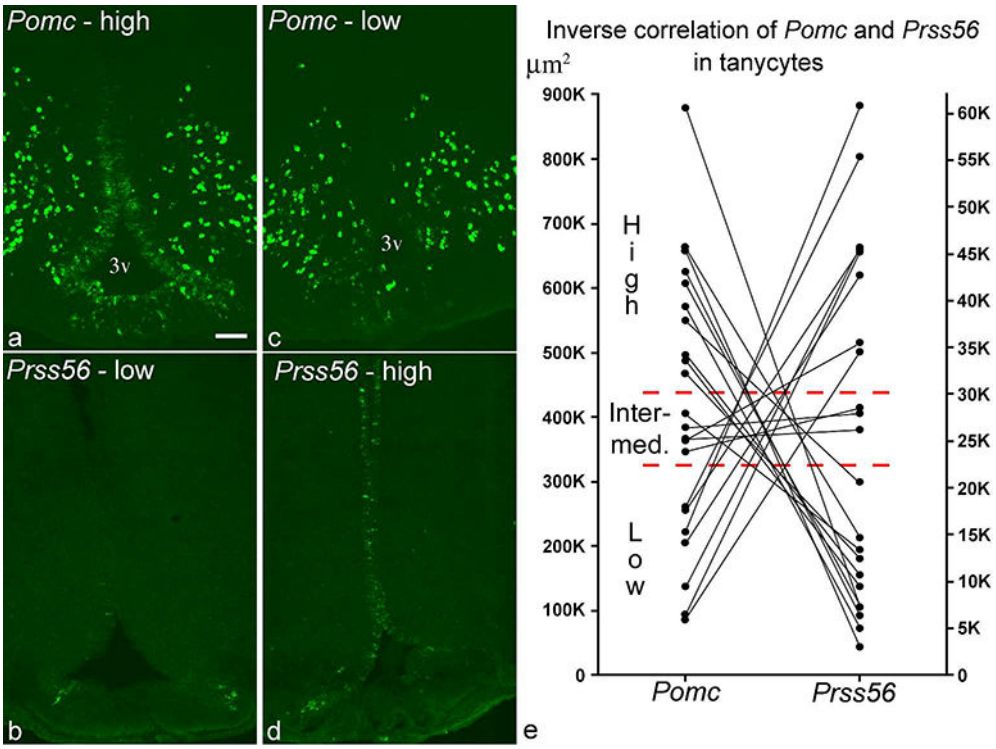

Figure 4.

(a, b) FISH performed on adjacent sections demonstrates a brain with high *Pomc* and low *Prss56,* (c, d) and another with low *Pomc* and high *Prss56* levels in tanycytes (rostrocaudal position: −3.4 mm from Bregma). 3v, third ventricle. Scale bar: 100µm. (e) Inverse correlation of *Pomc* and *Prss56* ISH signals in tanycytes from 22 adult rat brains. Y-axes represent area in μm^2 covered by hybridization signal. Indicated are the borders separating the qualitative categories of high, intermediate and low expression levels. Based on this quantification, one brain in Group 3 that had been classified as high *Pomc* in Wittmann et al. (2017) was re-classified as intermediate *Pomc.*

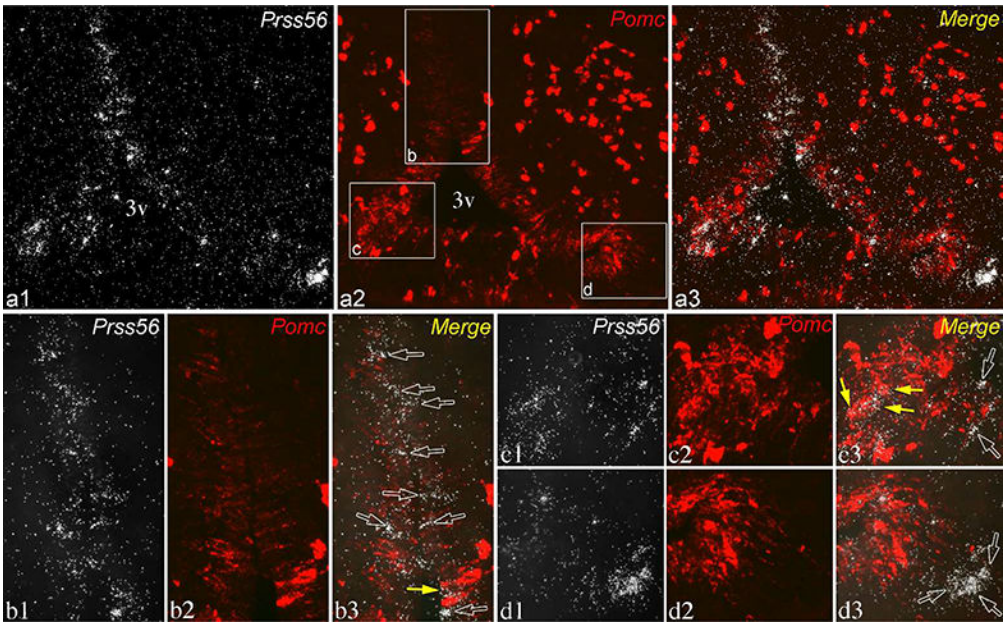

Figure 5.

Dual-label ISH for *Prss56* (silver grains, white) and *Pomc* (fluorescence, pseudocolored red) in a brain with intermediate expression levels in tanycytes for both transcripts. Section shown is close to level c2 in Fig. 2, from the same brain. (a1-a3) Lower magnification of the same field shows the distribution of *Prss56* and *Pomc* in tanycytes. Higher magnification images of boxed areas in a2 are shown in lower panels, b-d. (b1-b3) In the α2 tanycyte domain, most Prss56-expressing tanycytes are negative for *Pomc* (open arrows), although 1 or 2 are labeled with *Pomc* hybridization signal (yellow arrow). (c1-c3) In the β1 domain, *Prss56* hybridization signal concentrates over a few Pomc-expressing tanycytes (yellow arrows). (d1-d3) The group of γ tanycytes labeled for *Prss56* is negative for *Pomc* (open arrows). 3v, third ventricle. Scale bar: 100μm on a; 25μm on bl (for b-e).

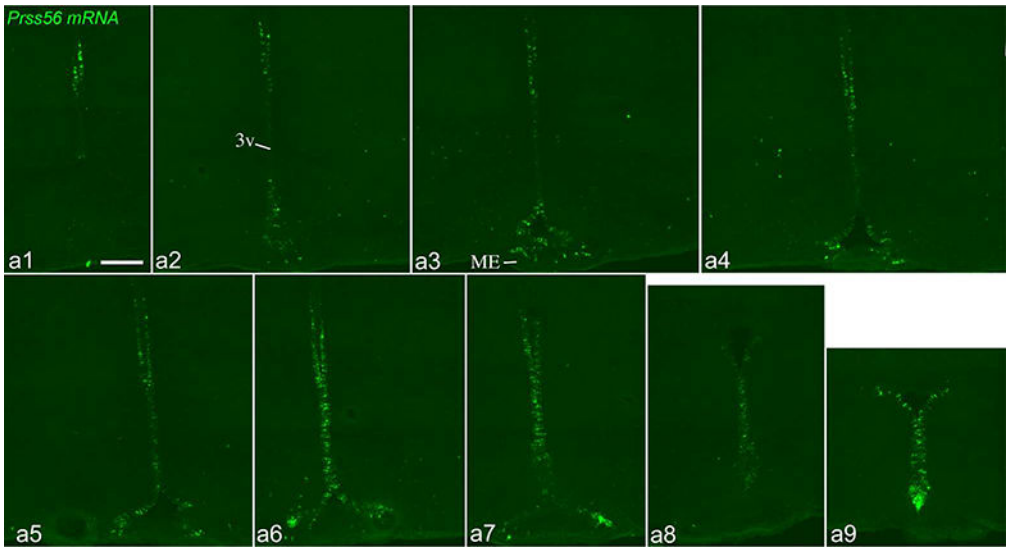

Figure 6.

Prss56 mRNA distribution by FISH in an adolescent, 32-day-old, male rat. Sections are arranged in rostro-caudal order (a1: most rostral; a9: most caudal), with ~200μm distance between consecutive sections. 3v, third ventricle; ME, median eminence. Scale bar: 200μm.

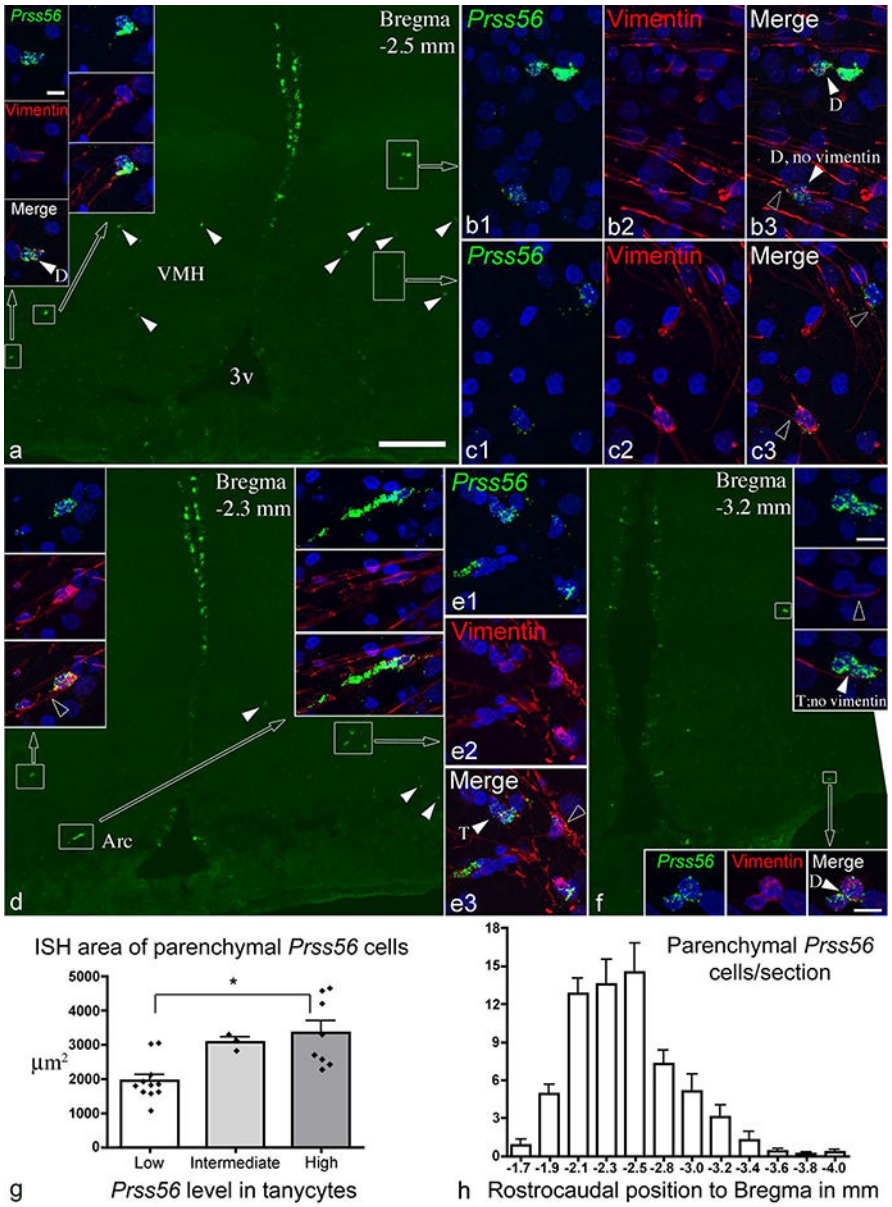

Figure 7.

(a, d, f) Distribution of Prss56-expressing parenchymal cells (arrowheads, boxed areas) in the ventromedial and arcuate nuclei. Sections are from male 15 week-old rats, one with high (a and d), another (f) with low *Prss56* levels in tanycytes. Cells in boxed areas are shown in high magnification in insets, and in b, c and e. Vimentin immunofluorescence is shown in red, nuclear DAPI signal in blue. Most, though not all, *Prss56* cells contain vimentin in their cytoplasm. In the high magnification images, white arrowheads indicate two (D) or three (T) closely adjacent *Prss56* cells; open arrowheads point to tanycyte processes adjacent to *Prss56* cells. (g) Quantification of FISH signal of parenchymal *Prss56* cells (n=22 rats), and compared between groups with low, intermediate and high *Prss56* in tanycytes; * $p<0.01$. (h) Rostrocaudal distribution of parenchymal *Prss56* cells, showing mean cell number per section (n=10 rats). 3v, third ventricle; Arc, arcuate nucleus; VMH, ventromedial nucleus.

Scale bars: 200 μm on a (for a, d, f); 10μm on top left inset (also for b, c, e and all insets except in f); 10μm on insets of f.

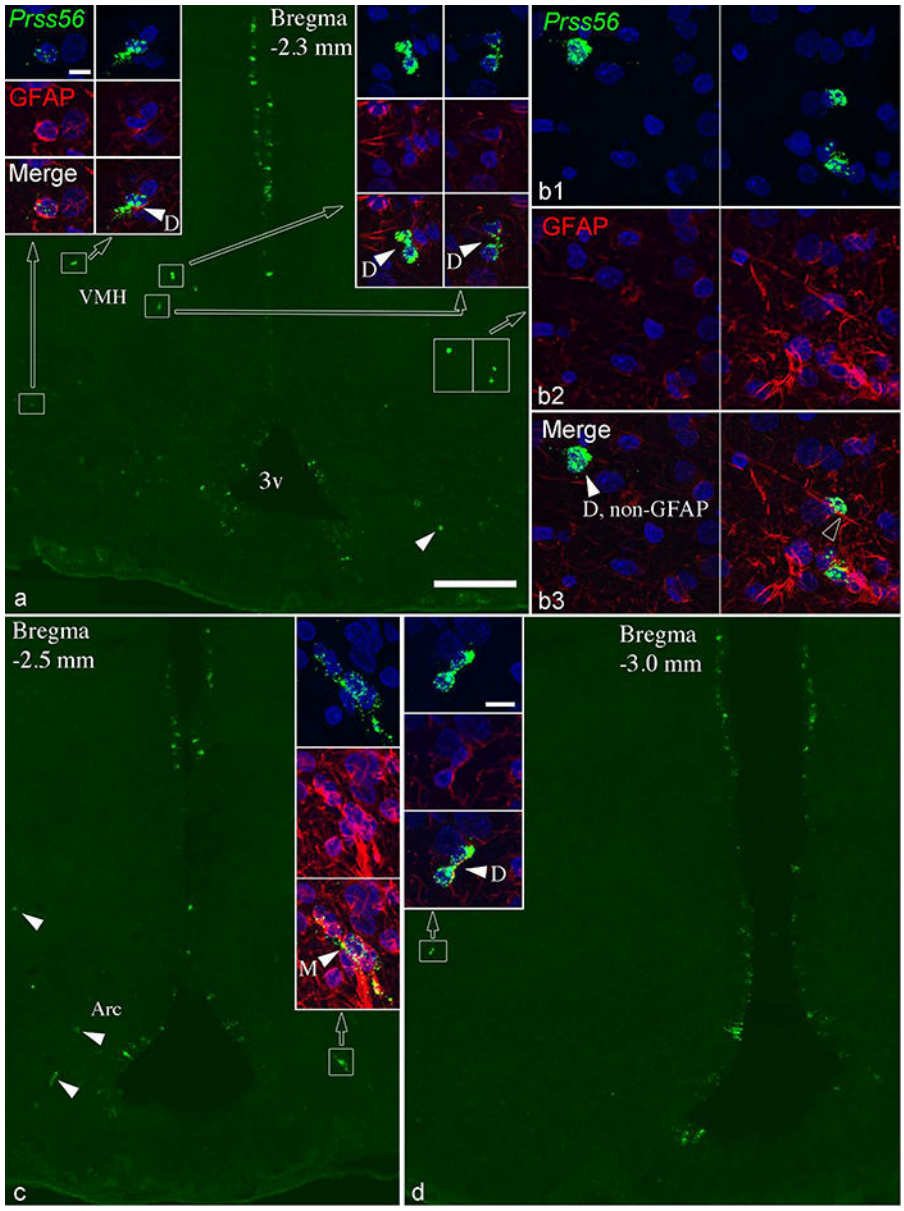

Figure 8.

Most parenchymal *Prss56* cells express GFAP. (a, c, d) Sections shown from two 15 week-old rats with high *Prss56* expression in tanycytes; parenchymal *Prss56* cells are in the boxed areas or indicated by arrowheads. Cells in boxed areas are shown in high magnification in insets, and in b. GFAP immunofluorescence is shown in red, nuclear DAPI signal in blue. Most, though not all, *Prss56* cells also contain GFAP. In the high magnification images, white arrowheads indicate two (D) or multiple (M) closely adjacent *Prss56* cells; open arrowheads point to tanycyte processes adjacent to *Prss56* cells. 3v, third ventricle; Arc, arcuate nucleus; VMH, ventromedial nucleus. Scale bars: 200 μm on a (for a, c, d); 10μm on top left inset (also for b, and all insets except in d); 10μm on inset of d.

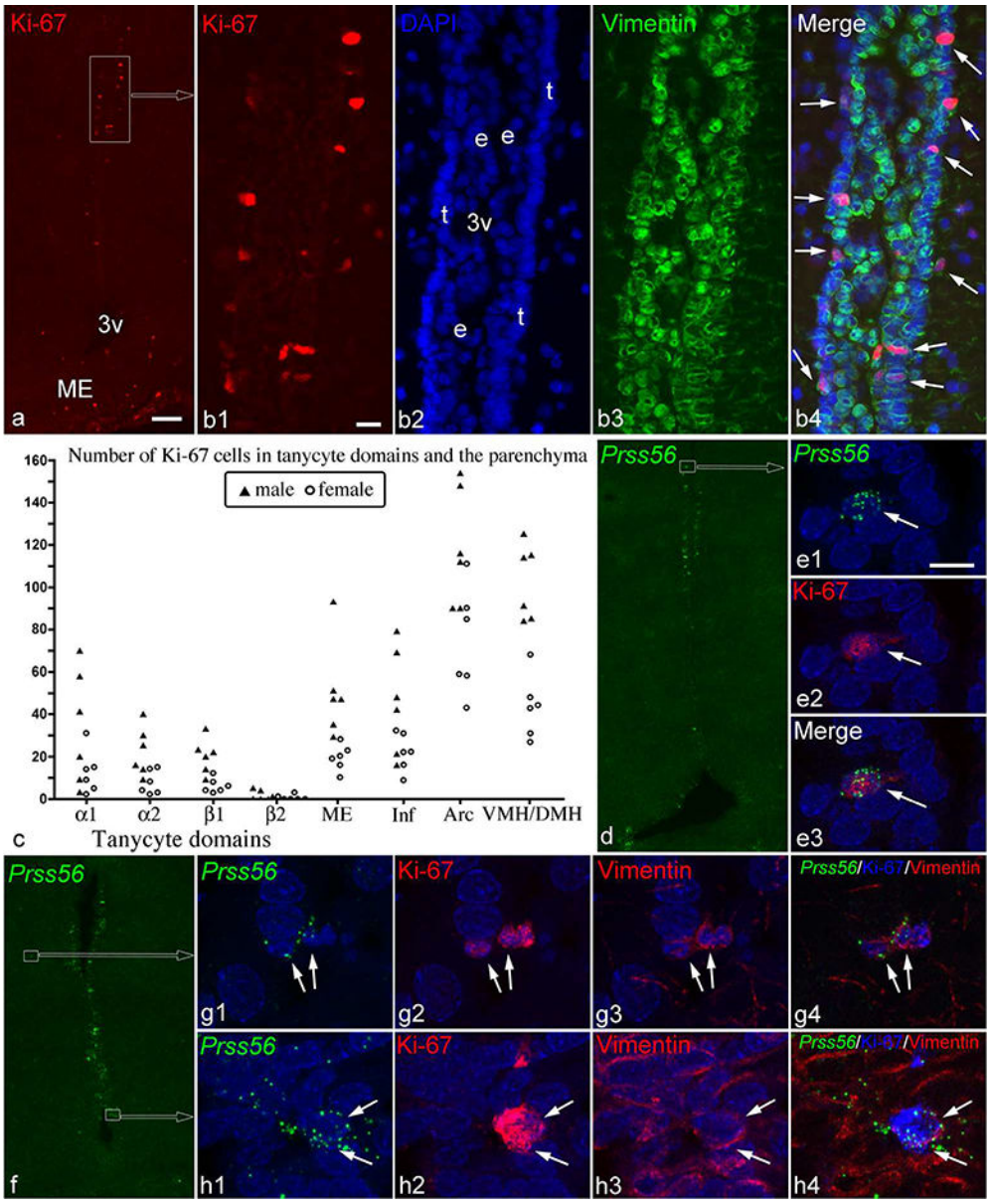

Figure 9.

(a) Ki-67 immunofluorescence demonstrates a highly proliferative zone in the α1 tanycyte domain (boxed area). (b1–4) Higher magnification images of this zone show that most Ki-67 cells are in the layer of tanycytes (t in B2, nuclear DAPI staining) facing the parenchyma, and express vimentin (green; arrows in b4). 3v, third ventricle; e, ependymal cell layers. (c) The number of Ki-67 cells shows large variations among 6 male and 6 female rats in tanycytic domains, the median eminence (ME), infundibular stalk (Inf), arcuate nucleus (Arc), and the ventromedial and dorsomedial nuclei (VMH/DMH). (d-h) Ki-67 in Prss56-expressing cells (white arrows), including an α1 tanycyte (d, e), parenchymal cells (f, g) and β1 tanycytes (f, h). Vimentin in the cytoplasm of the parenchymal cells and β1 tanycytes is shown in g3 and h3. Scale bar: 100μm in a (for a, d, f); 20μm in b; and 10μm in e1 (for e, g, h).

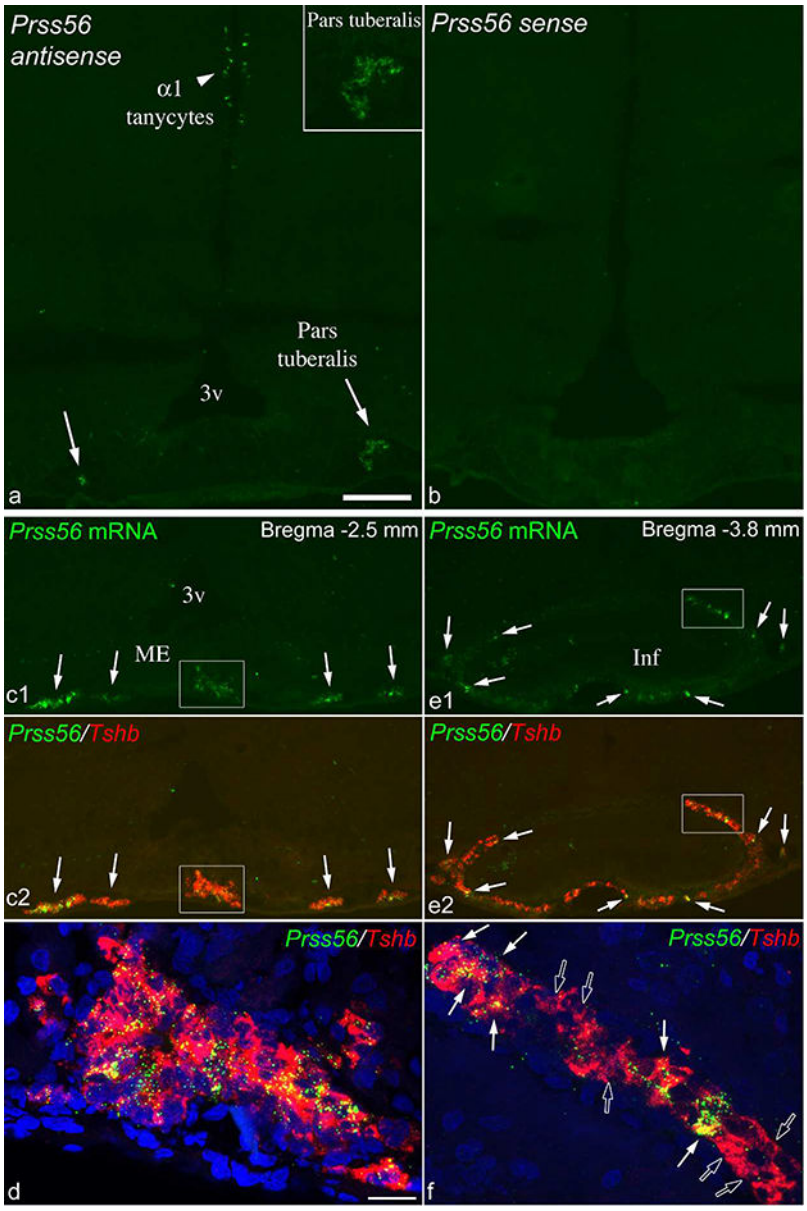

Figure 10.

Prss56 mRNA in the pars tuberalis of adult rats. (a) FISH for *Prss56* shows labeled cells in the pars tuberalis (arrows; right side magnified in inset) in a 15 week old rat that had high *Prss56* expression the pars tuberalis, and low in tanycytes. (b) FISH with the sense probe that was processed parallel on the adjacent section demonstrates the lack of labeling in the pars tuberalis and tanycytes. (c-f) Dual FISH for *Prss56* (green) and *Tshb* (red) on another 15 week old rat with high *Prss56* mRNA levels in the pars tuberalis and low in tanycytes. (cl, c2) Rostrally, *Prss56* mRNA is detected in almost all *Tshb* cells (arrows and boxed area). Confocal image of the boxed area is shown in d, with blue nuclear DAPI staining included. (el, e2) Caudally, *Prss56* mRNA was detected in only a portion of *Tshb* cells (arrows point to examples). Confocal image of the boxed area is shown in f. White arrows indicate *Tshb* cells that co-express *Prss56* mRNA, open arrows point to single-labeled *Tshb* cells. 3v, third

ventricle; Inf, infundibular stalk; ME, median eminence. Scale bar: 200μm on a (for a-c, and e); 20μm on d (for d and f).

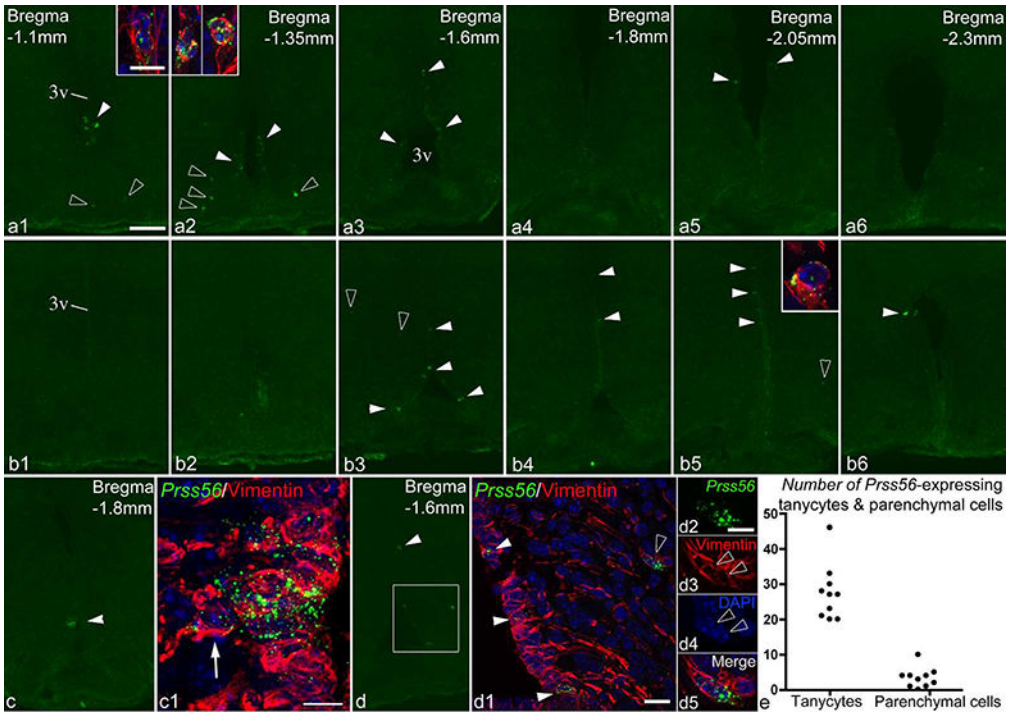

Figure 11.

Prss56 expression in the mouse hypothalamus. (a, b) FISH demonstrates *Prss56* mRNA-expressing cells in rostro-caudal series of sections from two male mice (a1–6 and b1–6). White arrowheads indicate Prss56-expressing tanycytes, open arrowheads point to parenchymal cells. Insets show high magnification confocal images of some of the parenchymal cells, with vimentin (red) and DAPI (blue) staining included. Note that insets in A1 and A2 show pairs of adjacent Prss56-expressing parenchymal cells. (c) *Prss56* expression localized to a small group of α2 tanycytes. (c1) High magnification confocal image (Z-projection) of this area shows a Prss56-expressing tanycyte (arrow) located outside the tanycyte layer. (d-d5) Confocal image (d1) of the boxed area in d shows *Prss56* mRNA in tanycytes (white arrowheads) and parenchymal cells (open arrowhead), the latter positioned adjacent and to vimentin-positive tanycyte processes (red). Magnified images of the parenchymal Prss56-expressing cells in d1-d4 demonstrate that these are two closely adjacent cells. (e) Cell counts of *Prss56*- expressing tanycytes and parenchymal cells from 10 adult mice. Cells were counted on 6–7 sections from each mouse. 3v, third ventricle. Scale bar: 100μm on a1 (for a1-a6, bl- b6, c, d); 10μm in inset of a1 (for all insets); 10μm in cl; 20μm in d1; 10μm in d2.

Table 1.

Four groups of adult rats were used in this study. In each group, rats were euthanized within 2h of the mid-day period but on different dates. *Prss56* expression was classified based on the quantification of FISH signal, as seen in Fig. 4.

Group #	Number of rats	Sex	Weight (g)	Age	*Prss56* expression		
					Low	Intermediate	High
Group 1	6	M	257–284	~8–9 weeks	2	0	4
Group 2	6	F	224–245	~9–10 weeks	4	1	1
Group 3	4	M	286–293	~9–10 weeks	3	1	0
Group 4	6	M	413–436	15 weeks	2	1	3